

SSC-190

**BENDING MOMENT DISTRIBUTION IN A  
MARINER CARGO SHIP MODEL IN  
REGULAR AND IRREGULAR WAVES  
OF EXTREME STEEPNESS**

**This document has been approved  
for public release and sale; its  
• distribution is unlimited.**

**SHIP STRUCTURE COMMITTEE**

# SHIP STRUCTURE COMMITTEE

## MEMBER AGENCIES:

UNITED STATES COAST GUARD  
NAVAL SHIP SYSTEMS COMMAND  
MILITARY SEA TRANSPORTATION SERVICE  
MARITIME ADMINISTRATION  
AMERICAN BUREAU OF SHIPPING

## ADDRESS CORRESPONDENCE TO:

SECRETARY  
SHIP STRUCTURE COMMITTEE  
U.S. COAST GUARD HEADQUARTERS  
WASHINGTON, D.C. 20591

November 1968

Dear Sir:

A Mariner ship-model study at Stevens Institute of Technology sponsored by the Ship Structure Committee has developed data to support the measurement of the maximum vertical wave-bending moment at the midship section of ships in both regular and irregular waves. Herewith is a copy of a report on the model study entitled *Bending Moment Distribution In A Mariner Cargo Ship Model In Regular And Irregular Waves Of Extreme Steepness* by Naresh M. Maniar and Edward Numata.

This report is being distributed to individuals and groups associated with or interested in the work of the Ship Structure Committee. Comments concerning this report are solicited.

Sincerely,



D. B. Henderson  
Rear Admiral, U. S. Coast Guard  
Chairman, Ship Structure Committee

SSC-190  
Final Report  
on  
Project SR-165  
"Bending Moment Determination"  
to the  
Ship Structure Committee

BENDING MOMENT DISTRIBUTION IN A MARINER CARGO SHIP MODEL  
IN REGULAR AND IRREGULAR WAVES OF EXTREME STEEPNESS

by  
Naresh M. Maniar  
and  
Edward Numata

Department of the Navy  
Naval Ship Engineering Center  
Contract Nobs 88263

This document has been approved  
for public release and sale; its  
distribution is unlimited.

U. S. Coast Guard Headquarters  
Washington, D. C.

November 1968

## ABSTRACT

An experimental investigation was undertaken to determine (1) the lengthwise vertical wave-bending-moment distribution within the midship half-length and (2) the relationship between bending moment and extreme wave steepness, for a MARINER-type cargo ship.

A 1/96-scale model was cut to form six segments, which were joined by a flexure beam. The beam was strain-gaged to measure bending moments at the hull cuts at stations 5,  $7\frac{1}{2}$ , 10,  $12\frac{1}{2}$ , and 15.

The model was tested with normal weight distribution and with an extreme "cargo amidship" loading in both head and following seas. The range of regular-wave steepness (height/length) was 0.05 to 0.11; the irregular waves had an equivalent full-size significant height of 39 feet.

Within practical operational limits of speed for the MARINER-type ship, the maximum wave bending moments in high regular waves were found to occur in the region from amidship to 0.125L aft of amidships. Thus the practice of concentrating on midship bending moments both in design studies and full-scale measurements appears to be justified for ships of the MARINER-type. Hogging and sagging moments at any section were found to be generally proportional to wave height, up to a wave-height to wavelength ratio of 0.11, the steepest wave that could be generated. The bending-moment and wave data from the test in irregular waves were processed by spectral analysis to obtain equivalent regular-wave responses. These were shown to be, generally, in good enough agreement with the bending-moment response obtained directly in regular waves to inspire confidence in the use of regular-wave response operators and spectral-analysis technique to predict the vertical wave bending moment of a ship in irregular waves.

## CONTENTS

	<u>Page</u>
INTRODUCTION .....	1
DESCRIPTION OF THE EXPERIMENT .....	2
ANALYSIS AND DISCUSSION .....	25
SUMMARY .....	32
CONCLUSIONS .....	32
RECOMMENDATION .....	32
ACKNOWLEDGEMENT .....	32
REFERENCES .....	33

## SHIP STRUCTURE COMMITTEE

The SHIP STRUCTURE COMMITTEE is constituted to prosecute a research program to improve the hull structures of ships by an extension of knowledge pertaining to design, materials and methods of fabrication.

RADM D. B. Henderson, USCG - Chairman  
Chief, Office of Engineering  
U. S. Coast Guard Headquarters

Captain William R. Riblett  
Head Ship Engineering Division  
Naval Ship Engineering Center

Mr. E. Scott Dillon  
Chief, Division of Ship Design  
Office of Ship Construction  
Maritime Administration

Captain T. J. Banvard, USN  
Maintenance and Repair Officer  
Military Sea Transportation Service

Mr. D. B. Bannerman, Jr.  
Vice President - Technical  
American Bureau of Shipping

## SHIP STRUCTURE SUBCOMMITTEE

The SHIP STRUCTURE SUBCOMMITTEE acts for the Ship Structure Committee on technical matters by providing technical coordination for the determination of goals and objectives of the program, and by evaluating and interpreting the results in terms of ship structural design, construction and operation.

### NAVAL SHIP ENGINEERING CENTER

Mr. J. J. Nachtsheim - Chairman  
Mr. John Vasta - Contract Administrator  
Mr. George Sorkin - Member  
Mr. Harrison Sayre - Alternate  
Mr. Ivo Fioriti - Alternate

### MARITIME ADMINISTRATION

Mr. Frank Dashnaw - Member  
Mr. Anatole Maillar - Member  
Mr. R. Falls - Alternate  
Mr. W. G. Frederick - Alternate

### AMERICAN BUREAU OF SHIPPING

Mr. G. F. Casey - Member  
Mr. F. J. Crum - Member

### OFFICE OF NAVAL RESEARCH

Mr. J. M. Crowley - Member  
Dr. Wm. G. Rauch - Alternate

### MILITARY SEA TRANSPORTATION SERVICE

LCDR R. T. Walker, USN - Member  
Mr. R. R. Askren - Member

### U. S. COAST GUARD

CDR C. R. Thompson, USCG - Member  
LCDR R. L. Prown, USCG - Alternate  
LCDR James L. Howard, USCG - Alternate  
LCDR Leroy C. Melberg, USCG - Alternate

### NAVAL SHIP RESEARCH & DEVELOPMENT CENTER

Mr. A. B. Stavovy - Alternate

## LIAISON REPRESENTATIVES

### NATIONAL ACADEMY OF SCIENCES- NATIONAL RESEARCH COUNCIL

Mr. A. R. Lytle - Technical Director, MTRB

Mr. R. W. Rumke - Executive Secretary, SRC

### AMERICAN IRON AND STEEL INSTITUTE

Mr. J. R. LeCron

### BRITISH NAVY STAFF

Mr. H. E. Hogben  
Staff Constructor Officer Douglas  
Faulkner, RCNC

### WELDING RESEARCH COUNCIL

Mr. K. H. Koopman, Director  
Mr. Charles Larson, Secretary

LIST OF FIGURES

1.	Model Drawing . . . . .	2
2.	Structural Beam . . . . .	4
3.	Weight Distribution and Still-Water Bending Moments . . . . .	5
4.	Filter Response . . . . .	7
5.	Irregular Wave Spectrum . . . . .	9
6.	Bending Moments Variation Along the Model Length, Model 2681-2. Model Heading $180^{\circ}$ ; Froude No. = .12 to .14; Wave Length 0.75L . . . . .	11
7.	Bending Moments Variation Along the Model Length, Model 2681-2. Model Heading $180^{\circ}$ ; Froude No. = .13 to .14; Wave Length 1.00L . . . . .	11
8.	Bending Moments Variation Along the Model Length, Model 2681-2. Model Heading $180^{\circ}$ ; Froude No. = .13 to .15; Wave Length 1.25L . . . . .	12
9.	Bending Moments Variation Along the Model Length, Model 2681-2. Model Heading $180^{\circ}$ ; Froude No. = .12 to .14; Wave Length 1.50L . . . . .	12
10.	Bending Moments Variation Along the Model Length, Model 2681-2. Model Heading $180^{\circ}$ ; Froude No. = .13 to .14; Wave Length 1.75L . . . . .	12
11.	Bending Moments Variation Along the Model Length, Model 2681-2. Model Heading $180^{\circ}$ ; Froude No. = 0; Wave Length 0.75L . . . . .	12
12.	Bending Moments Variation Along the Model Length, Model 2681-2. Model Heading $180^{\circ}$ ; Froude No. = 0; Wave Length 1.00L . . . . .	13
13.	Bending Moments Variation Along the Model Length, Model 2681-2. Model Heading $180^{\circ}$ ; Froude No. = 0; Wave Length 1.25L . . . . .	13
14.	Bending Moments Variation with Wave Height, Model 2681-2. Model Heading $180^{\circ}$ ; Froude No. = 0; Wave Length 1.25L . . . . .	13
15.	Bending Moments Variation Along the Model Length, Model 2681-2. Model Heading $180^{\circ}$ ; Froude No. = 0; Wave Length 1.50L . . . . .	13
16.	Bending Moments Variation Along the Model Length, Model 2681-2. Model Heading $180^{\circ}$ ; Froude No. = 0; Wave Length 1.75L . . . . .	14
17.	Bending Moments Variation Along the Model Length, Model 2681-2. Model Heading $180^{\circ}$ ; Froude No. = Drift, -.09 to -.12; Wave Length 0.75L . . . . .	14
18.	Bending Moments Variation Along the Model Length, Model 2681-2. Model Heading $180^{\circ}$ ; Froude No. = Drift, -.09 to -.12; Wave Length 1.00L . . . . .	14
19.	Bending Moments Variation Along the Model Length, Model 2681-2. Model Heading $180^{\circ}$ ; Froude No. = Drift; Wave Length 1.25L . . . . .	14

20.	Bending Moments Variation Along the Model Length, Model 2681-2. Model Heading $180^{\circ}$ ; Froude No. = Drift, $-.11$ to $-.13$ ; Wave Length $1.50L$ . . . . .	15
21.	Bending Moments Variation Along the Model Length, Model 2681-2. Model Heading $180^{\circ}$ ; Froude No. = Drift, $-.12$ to $-.13$ ; Wave Length $1.75L$ . . . . .	15
22.	Bending Moments Variation Along the Model Length, Model 2681-2. Model Heading $0^{\circ}$ ; Froude No. = $.18$ ; Wave Length $0.75L$ . . . . .	15
23.	Bending Moments Variation Along the Model Length, Model 2681-2. Model Heading $0^{\circ}$ ; Froude No. = $.20$ to $.22$ ; Wave Length $1.00L$ . . . . .	15
24.	Bending Moments Variation Along the Model Length, Model 2681-2. Model Heading $0^{\circ}$ ; Froude No. = $.21$ to $.23$ ; Wave Length $1.25L$ . . . . .	16
25.	Bending Moments Variation Along the Model Length, Model 2681-2. Model Heading $0^{\circ}$ ; Froude No. = $.22$ to $.23$ ; Wave Length $1.50L$ . . . . .	16
26.	Bending Moments Variation Along the Model Length, Model 2681-2. Model Heading $0^{\circ}$ ; Froude No. = $.20$ to $.21$ ; Wave Length $1.75L$ . . . . .	16
27.	Location of Bending Moments Maxima, Model 2681-2 . . . . .	17
28.	Maximum Bending Moments Variation with Wave Length, Model 2681-2. Wave Height/Wave Length, $.05$ . . . . .	18
29.	Maximum Bending Moments Variation with Wave Length, Model 2681-2. Wave Height/Wave Length, $.07$ . . . . .	19
30.	Maximum Bending Moments Variation with Wave Length, Model 2681-2. Wave Height/Wave Length, $.10$ . . . . .	20
31.	Bending Moments Variation with Wave Steepness, Model 2681-2. Station 5 . . . . .	21
32.	Bending Moments Variation with Wave Steepness, Model 2681-2. Station $7\frac{1}{2}$ . . . . .	22
33.	Bending Moments Variation with Wave Steepness, Model 2681-2. Station 10 . . . . .	23
34.	Bending Moments Variation with Wave Steepness, Model 2681-2. Station $12\frac{1}{2}$ . . . . .	24
35.	Bending Moments Variation with Wave Steepness, Model 2681-2. Station 15 . . . . .	25
36.	Comparison of Bending Moment Responses, Normal Weight Distribution . . . . .	26
37.	Comparison of Bending Moment Responses, Cargo-Amidship Weight Distribution . . . . .	27
38.	Bending Moments Variation with Wave Height, Model 2681-1 . . . . .	30
39.	Bending Moment vs. Wave Encounter Frequency, Model 2681-1 . . . . .	31



LIST OF TABLES

1. Model Characteristics . . . . .	3
2. Model-Segment Properties . . . . .	3
3. Test Program . . . . .	8

SYMBOLS

$h$	wave height, crest to trough, ft
$I$	weight moment of inertia, lb-in. <sup>2</sup>
$L$	model length on 20 stations, ft
LCB	longitudinal center of buoyancy
LCG	longitudinal center of gravity
RAO	response amplitude operator
$S_w, S_M$	spectral densities of wave and moment, respectively
$v/\sqrt{gL}$	Froude number
$\lambda$	wave length, ft
$\mu_s, \mu_h$	bending moment coefficients, sag and hog respectively
$\emptyset$	midship section, station 10

## INTRODUCTION

In 1960 the Ship Structure Committee authorized work on a research program entitled "Bending Moment Determination," which used model tests to investigate hull bending moments in regular waves of extreme steepness.

An earlier pilot program involving a T-2 tanker model had indicated that the midship bending moment might have an upper limit in waves less steep than the waves of the theoretically calculated maximum height/length ratio of 0.14.<sup>1</sup> It was concluded that the subject of bending moments in extreme high waves should be explored by testing quite different hull forms such as a destroyer, a tanker, and a dry cargo vessel, with variations in freeboard and weight distribution. Ship Structure Committee Project SR-157 covered those model tests, whose purpose was to obtain the midship bending moments in extreme waves.<sup>2,3</sup> The cargo vessel selected for this project was a standard MARINER, which is fairly representative of modern freighters.

Project SR-157 concluded that, within practical operational and design limits for commercial ships, no dramatic upper limit of wave bending moments at amidships is to be expected as wave-height/wave-length increases to a value of about 0.11.

Since this conclusion was limited to midship bending moments only, and it was known that maximum moments under certain circumstances could occur elsewhere, the investigations were extended to determining longitudinal distribution of moments in extreme waves. These investigations came under Project SR-165 and extended over the calendar years 1963 and 1964. At the end of 1963, the first progress report on Project SR-165 was presented as Report SSC-163.<sup>4</sup> The investigations reported here represent the work for the year 1964.

The model selected for SR-165 was that of the MARINER cargo ship with a normal weight distribution and with an extreme cargo-amidship loading. It was to be tested in essentially the same wave program used in the earlier experiments. The purpose of investigating the cargo-amidship case was to study the effect of a significant reduction in longitudinal gyradius on bending moments. The model was segmented and held together by a flexure beam. The beam was strain-gaged at stations 5,  $7\frac{1}{2}$ , 10,  $12\frac{1}{2}$ , and 15, to measure vertical bending moments.

During 1963 the model with a normal weight distribution was tested at forward speed, zero speed, and drift speed, in head seas; and with forward speed in following seas. The cargo-amidship condition was tested at zero speed in head seas. The tests were performed in regular waves where the wave-length/ship-length ratios ranged from 0.75 to 1.75 and the wave-height/wave-length ratios ranged from 0.05 to 0.11.

The conclusions of the 1963 investigations were as follows:

- (1) Within the practical operational limits of ship speed in head and following waves, for the MARINER, the maximum wave bending moments in extreme regular waves occur in the region from amidships to 0.125L aft of amidships.
- (2) Hogging and sagging wave bending moments at any section are generally proportional to wave height -- up to a wave-height/wave-length ratio of 0.11, the steepest wave that could be generated.

The latter conclusion substantiated the findings of Project SR-157.

The program for 1964 was as follows:

- (1) Completion of the tests for the cargo-amidship case in regular waves.
- (2) Testing of both models in realistic irregular waves, and comparison of the

results with those from the regular-wave tests.

- (3) Hypothesizing on why, in the 1963 results, a double reversal appeared in the variation of bending moment along the model length in the head seas, drift-speed case; and in the following-seas forward-speed case.

DESCRIPTION OF THE EXPERIMENT

Model

The tests were conducted on a 65-inch (1/96-scale) six-segment fiberglass model of the standard MARINER, with a normal weight distribution and with a cargo-amidship loading. These two model conditions are designated 2681-1 and 2681-2, respectively. Figure 1 shows the body plan and model layout. Tables 1 and 2 contain the model

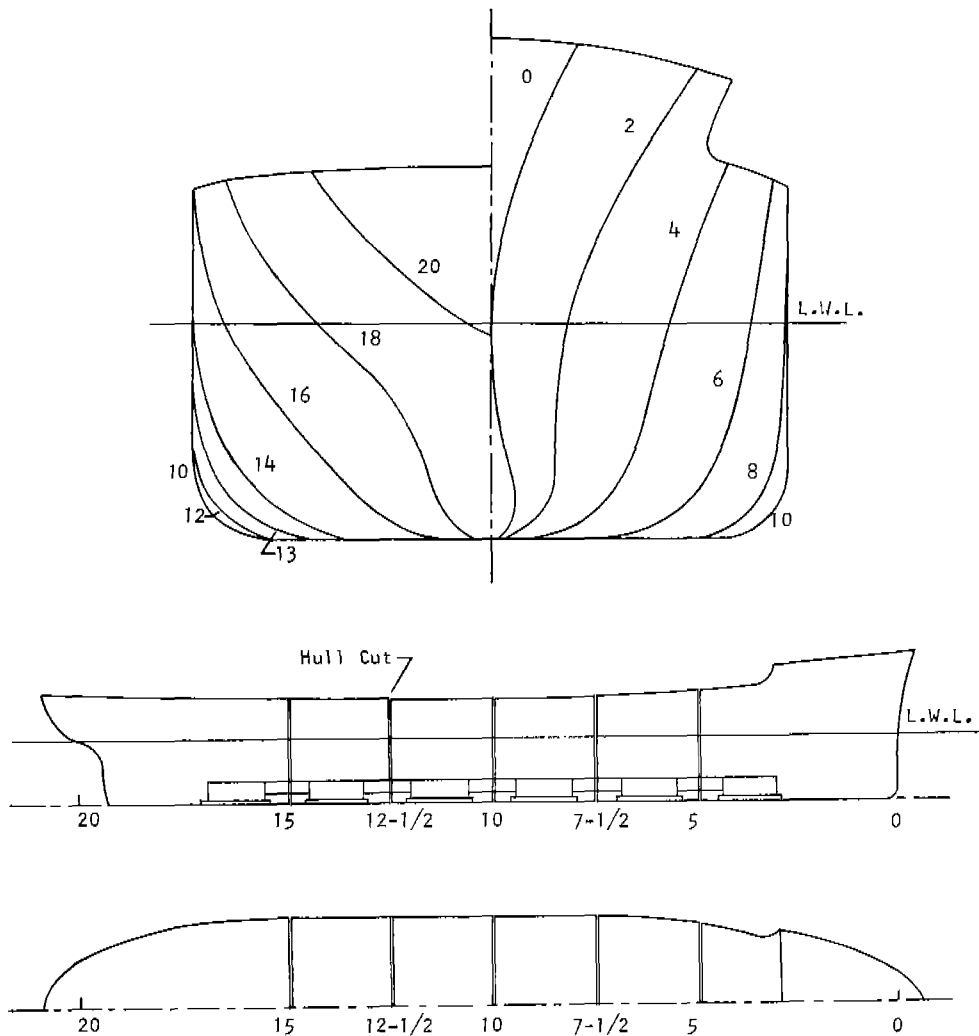


Fig. 1 Model Drawing

TABLE 1  
MODEL CHARACTERISTICS

Scale	1:96
Length on 20 stations, in.	65
Beam, in.	9.5
Draft, in.	3.47
Beam/Draft	2.72
Block Coefficient	0.61
Midship Section Coefficient	0.98

Model condition	2681-1	2681-2
Weight distribution	Normal	Cargo $\emptyset$
LCB, % ship length from $\emptyset$	1.44 aft	1.42 aft
Gyradius, % ship length	24.3	19.5

TABLE 2  
MODEL-SEGMENT PROPERTIES

Model 2681-1					Model 2681-2		
Segment	Wt. (lb)	LCG From $\emptyset$ (in.)	I About Seg. LCG (lb in. <sup>2</sup> )	$\frac{I \text{ Actual}}{I \text{ Req'd}}$	Wt. (lb)	LCG From $\emptyset$ (in.)	I About Seg. LCG (lb in. <sup>2</sup> )
1	8.04	23.29F	165	1.17	5.33	22.75F	157
2	6.50	11.95F	38	1.23	4.32	12.06F	35
3	8.17	3.99F	45	1.10	10.63	2.81F	83
4	8.34	3.91A	53	1.32	18.22	3.87A	111
5	7.49	12.31A	39	1.08	4.45	12.00A	37
6	9.84	22.18A	168	1.04	5.45	22.78A	163

characteristics and segment properties, respectively. The hull was cut at stations 5, 7 $\frac{1}{2}$ , 10, 12 $\frac{1}{2}$ , and 15. The segments were joined together by an aluminum flexure beam, which was bolted to aluminum plates imbedded in the segment bottoms. The hull cuts were 0.125-inch wide and sealed with 0.008-inch-thick rubber fixed to the hull with vinyl plastic electrical tape. An accordion fold was put into the sealing rubber to ensure that it would not contribute to hull stiffness.

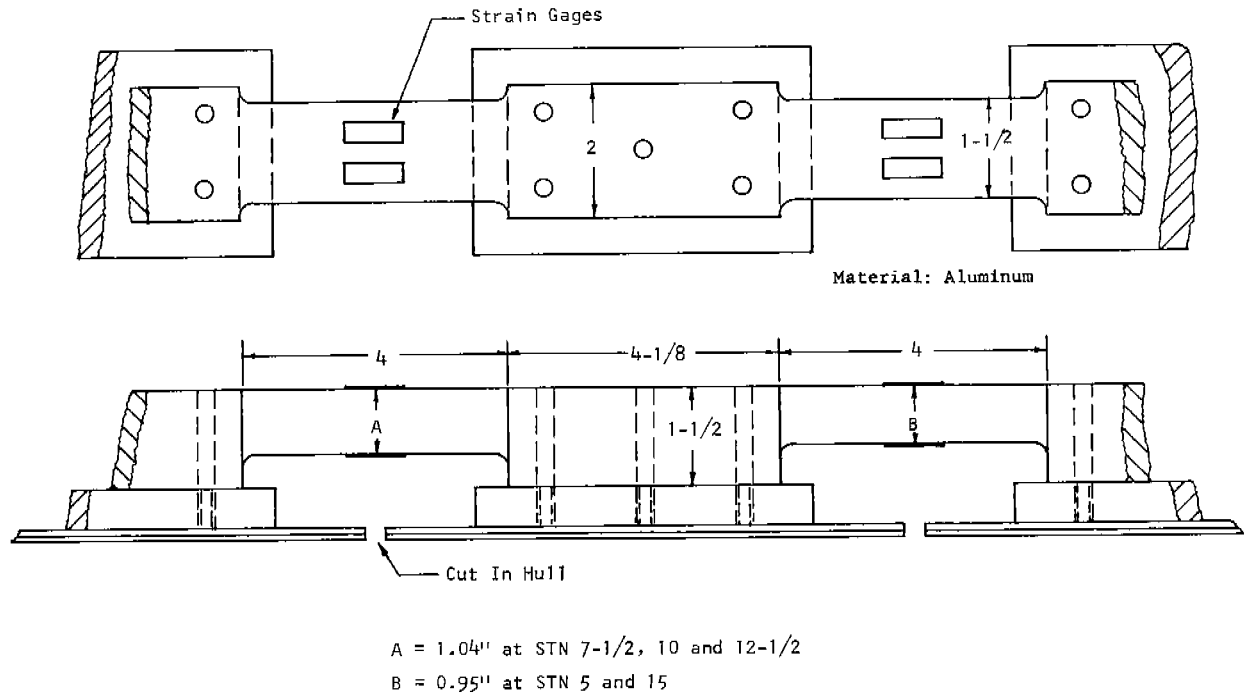


Fig. 2 Structural Beam.

The model was completely decked over except for a small hatch in the segment between stations 10 and 12 $\frac{1}{2}$ , necessary for accommodation of the towing gear and strain-gage wiring.

Figure 2 is the structural-beam drawing. The beam had six flexure sections, located centrally about the hull cuts. The flexures were 4-inches long and 1.5-inches wide; they were 1.04-inches deep at stations 7 $\frac{1}{2}$ , 10, and 12 $\frac{1}{2}$  and 0.95-inches deep at stations 5 and 15. The beam moment of inertia was made larger than the scaled-down value of ship inertia. This was done so that the fundamental vibration frequency of the model would be appreciably larger than the encounter frequency, and hence less likely to be a source of noise in the bending-moment record.

The model weight distributions are given in Fig. 3. In order to obtain the weight distribution for Model 2681-1, the normal weight distribution of the ship was divided into six parts corresponding to the six segments of the model. The weight, longitudinal center of gravity, and moments of inertia for each part were calculated and reduced to model scale. It was possible to ballast each segment to its required weight and LCG, but the moment of inertia was somewhat larger than required. In Table 2 the ratio  $I_{\text{actual}}/I_{\text{required}}$  is given for each segment. The influence of the excess segment inertias on the over-all inertia of the model was negligible. The weight of the towing gear located in the segment immediately aft of amidships was considered part of the ballast weight. Model 2681-2 was ballasted to obtain as small a longitudinal gyradius as possible.

#### Apparatus

The experiment was conducted in the Davidson Laboratory's Tank 3 (300' x 12' x 5.5').

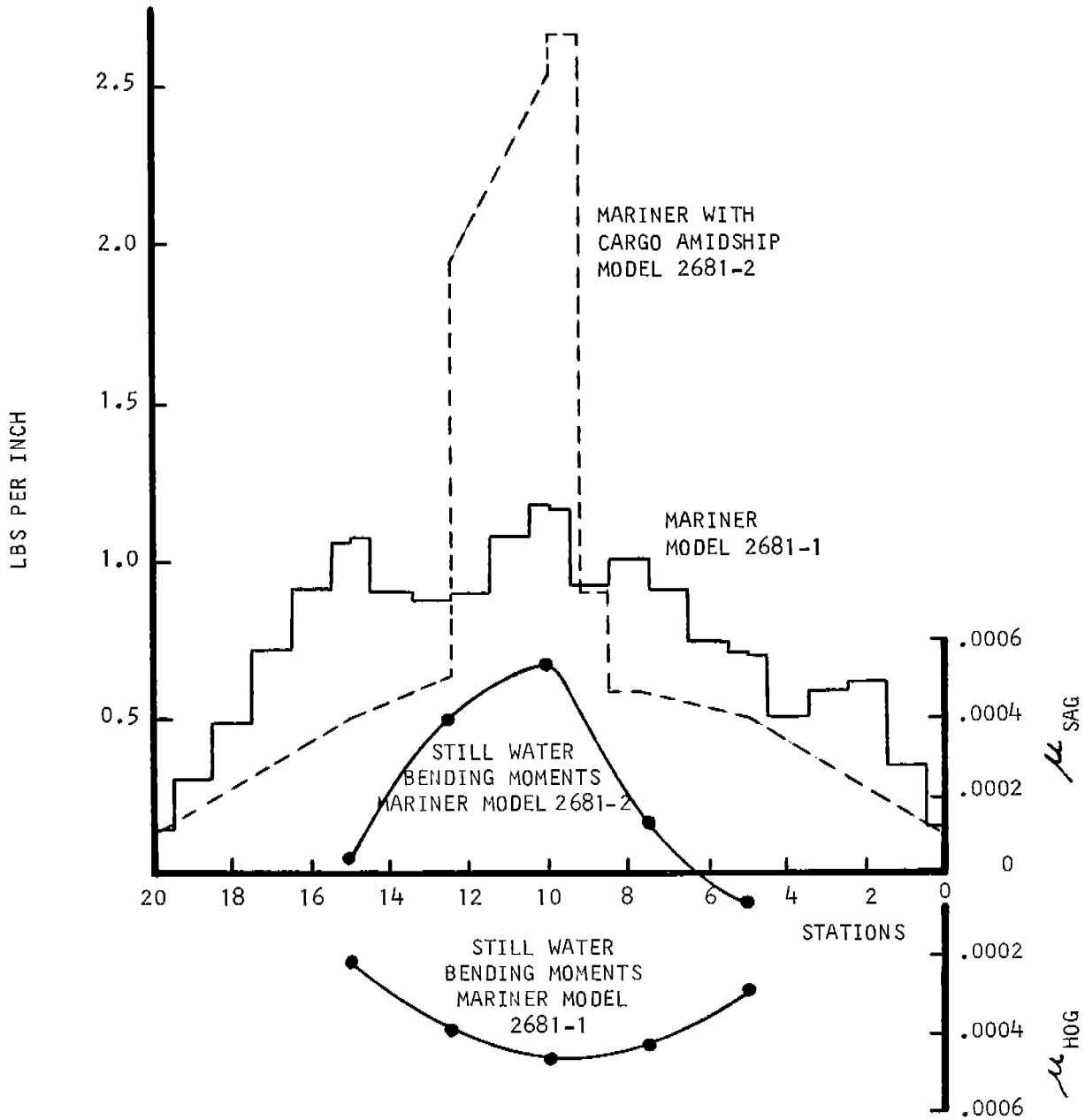


Fig. 3 Weight Distribution And Still Water Bending Moments.

The model was attached to a towing apparatus which gave it freedom to pitch, heave, and surge ( $\pm 6$  ft) but restrained it in roll, yaw, and sway. The apparatus consisted of a main carriage attached to the towing cable. The model was connected by a heave mast to a sub-carriage on the rail. The towing mast was permitted only vertical translational motion guided by ball-bearing rollers, and the sub-carriage had only fore and aft translational motion. The model was attached to the bottom

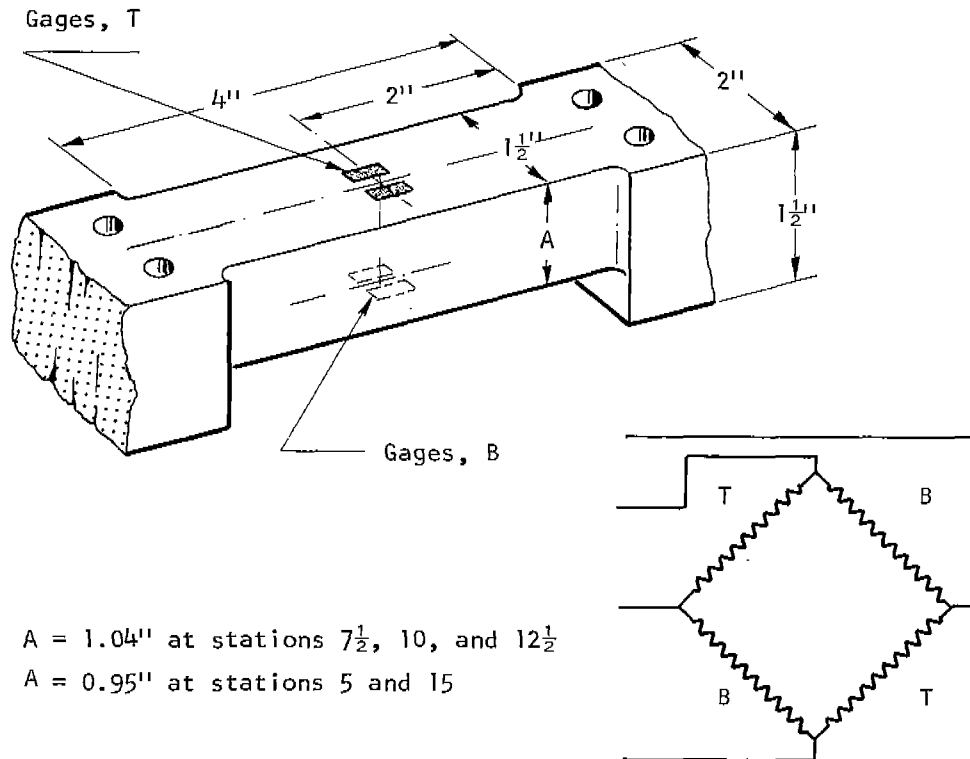
of the heave mast by pivots with an athwartship axis which allowed the model to pitch while restraining it in roll.

The model was run at forward speed by applying a known towing force to the sub-carriage through the use of falling weights placed at the end of a string which was led over a pulley system fixed to the main carriage. The main-carriage speed, controlled by a servo loop, was matched with the model speed. The towing weights were disconnected automatically at the end of the run, and the model slowed of its own accord.

The recording-run length was about four model lengths, over which the model moved with constant speed. A continuous speed record was obtained by a tachometer and a roller, fixed to the model sub-carriage. The average speed was obtained by measuring the time elapsed between two points 20-feet apart.

The 2-foot-long wave probe was of the resistance type, and designed for use in a plus or minus 6-inch wave-amplitude range. The probe was linear over the wave-amplitude range covered in the test. The static-calibration data points deviated from a straight-line plot less than 1 percent of the range of calibration. The probe was located 11 feet, 2 inches forward of the null surge position of the model.

Bending moments were determined from bending strains measured by SR-4, A-19 type strain gages. The moments in the beam were measured at stations 5,  $7\frac{1}{2}$ , 10,  $12\frac{1}{2}$ , and 15 (the locations of the hull cuts). A typical layout of gages on the flexure at each measuring station is shown in the sketch which appears below.



The four gages together formed a full Wheatstone-bridge circuit, registering bending strains only.



The beam, before installation in the model, was calibrated statically by the application of known moments. Each set of gages proved to have linear outputs, and there was no indication of metal hysteresis. At the start of each test day, each of the five sections of the flexure beam underwent a check calibration. A range of moment couples was applied through a system of adjustable weights.

In order to minimize high-frequency noise in the bending-moment record, active electronic filters were introduced in the electrical circuit, between the carrier amplifiers and the pen recorders. Because only four active filters were available, the moment at station 15 was unfiltered, since it was the least likely to experience high-frequency noise. The filter-response curve is presented in Fig. 4.

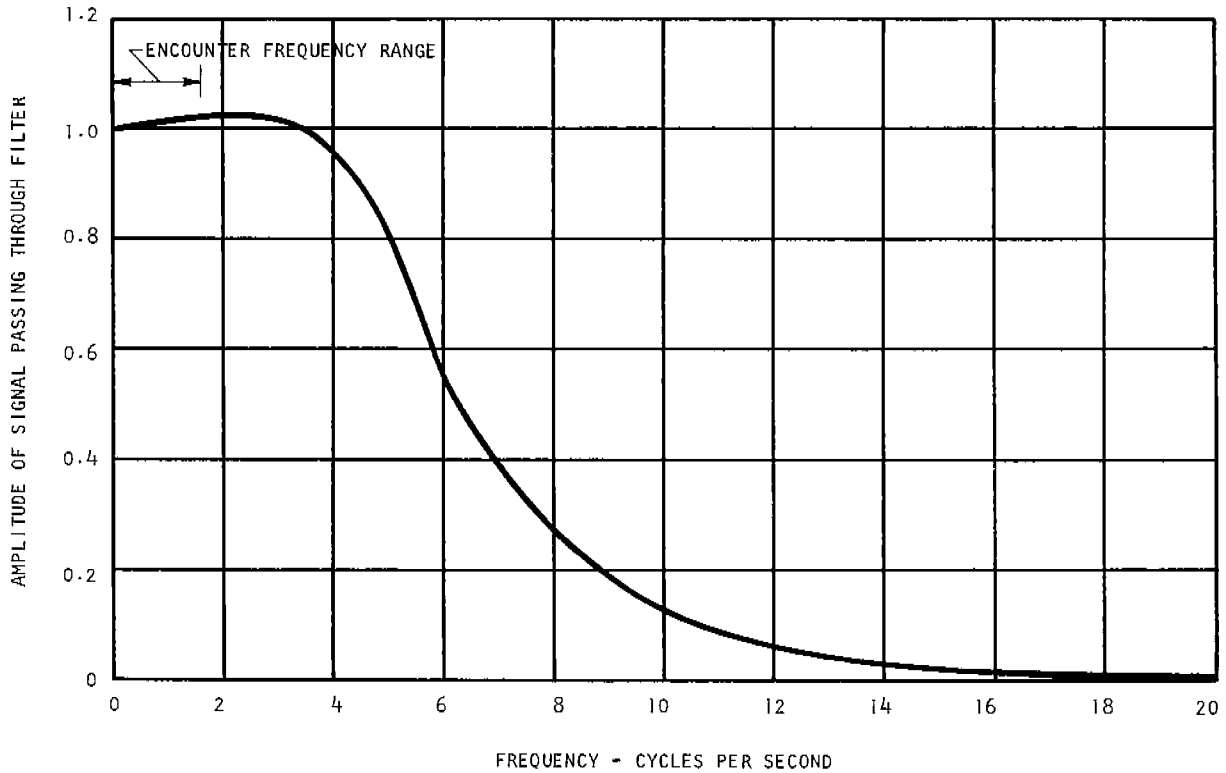


Fig. 4 Filter Response.

The outputs of the strain gages and of the wave wire were amplified by pre-amplifiers with a carrier frequency of 2400 cps and 4.5 volts rms. The outputs were recorded by a Sanborn pen writer on chart paper. For the tests in irregular waves, all six channels of information were recorded on magnetic tape as well as on chart paper.

#### Test Program

The test program was composed of regular wave tests of Model 2681-2 (cargo amidship) and irregular wave tests of both the models. The outline of the program appears in Table 3, which lists heading and speed combinations, and the waves in which the models were tested.

TABLE 3  
TEST PROGRAM

Wave Heights, Model 2681-2 in Regular Waves

Heading Speed	Wave Length/Model Length				
	0.75	1.00	1.25	1.50	1.75
180° forward	5	5	5	5	3
180° zero	5	-	-	-	- *
180° drift	5	5	5	5	3
0° forward	5	5	5	5	3

High Irregular Waves for Models 2681-1 and 2681-2

<u>Heading</u>	<u>Speed</u>	<u>No. of Runs</u>
180°	Forward	2
180°	Zero	1
180°	Drift	2
0°	Forward	2

\*Tests in wave lengths from 1.00L to 1.75L were performed in 1963.

In the case of the regular waves, the ratios of nominal wave length to model length covered by the program were 0.75, 1.00, 1.25, 1.50, and 1.75. The ratios of nominal wave height to wave length covered were 0.05, 0.07, 0.09, 0.10, and 0.11. In waves of  $\lambda/L \approx 1.75$ , the capacity of the wave-maker limited the wave height to  $h/\lambda \approx 0.09$ .

The test-program table refers to speed as forward, zero, or drift; but the actual speed in terms of Froude number appears at the head of the data curves.

The term "drift speed" needs qualification. For each wave length, the speed aimed at was the speed at which the model was run in the previous investigation by Dalzell.<sup>2</sup> Dalzell established the drift speed for all waves of the same length as the speed at which the MARINER model drifted astern in the highest wave associated with the particular wave length. In lower waves that speed was maintained by applying reverse thrust on the model.

The properties of the reproducible, irregular, long-crested waves employed in the test are listed below.

Sea State : High 7

Average Period, sec	12.6
Average Height, ft	26

Average of 1/3 Highest Heights, ft 39

Average of 1/10 Highest Heights, ft 47

Figure 5 shows the measured energy spectrum of these waves; a Pierson-Moskowitz spectrum having the same significant wave height is included for comparison. The Pierson-Moskowitz formulation has been adopted in the United States and foreign nations as an interim standard for typical sea spectra.

At zero speed the run length was sufficient to obtain an adequate statistical sample. At each forward and drift speed, two runs were taken to obtain an adequate sample. Speeds were averaged over a run length of 150 feet.

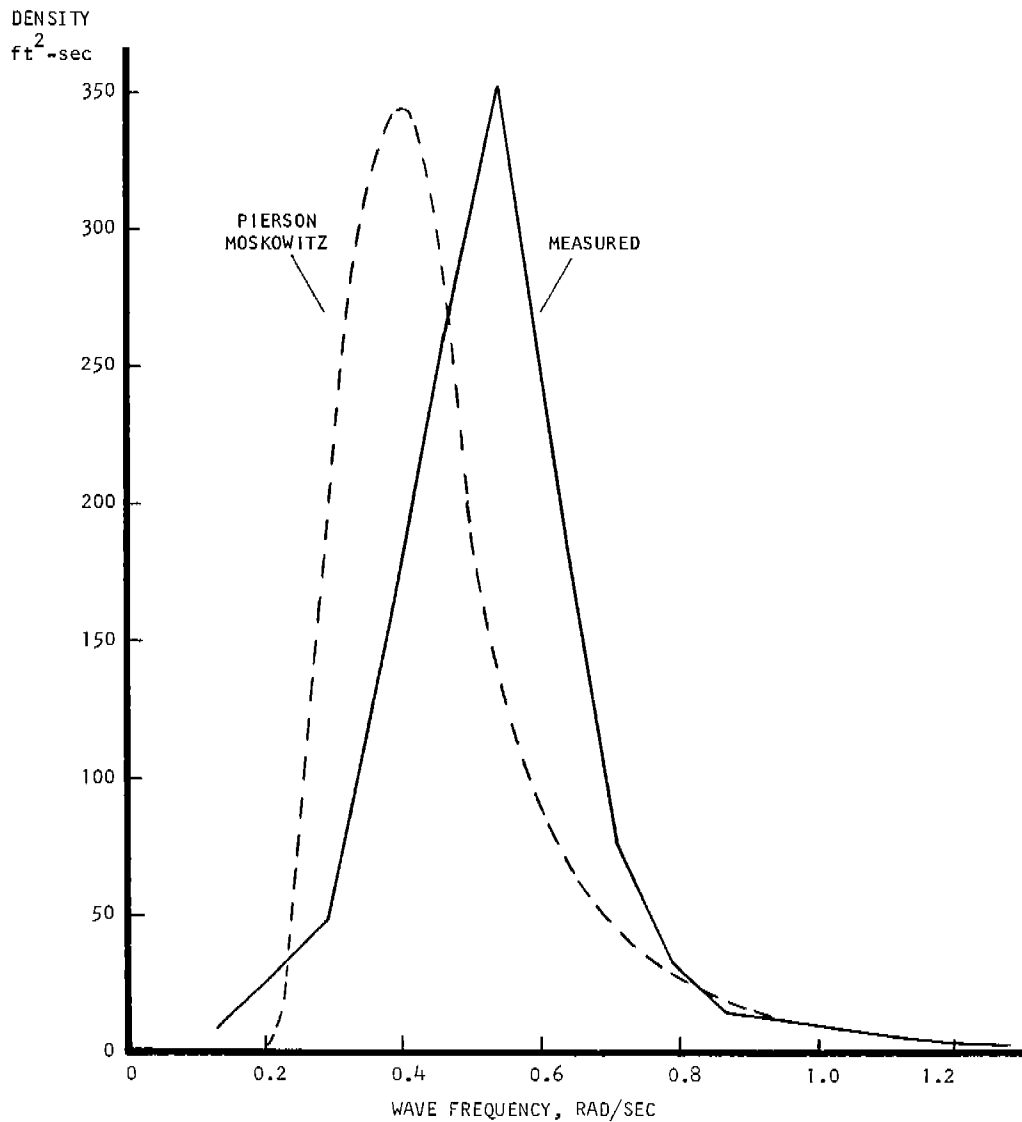


Fig. 5 Irregular Wave Spectrum.

Data Reduction

Regular-Wave Test

The magnitudes of wave heights and bending moments for each model run were obtained by averaging the data recorded for 20 feet of model travel. In the case of zero speed the averaging was performed for 20 cycles of the time history. At forward speed the number of cycles depended on the model speed, as noted in the outline which follows.

Head seas, forward speed	10-20 cycles
Head seas, drift speed	10-15 cycles
Following seas, forward speed	5-10 cycles

For waves, measurements were made of the double amplitude. For bending moments, measurements were made of the maxima of both hog and sag moments from still-water zero. These moments were exclusive of high-frequency noise and whipping moments. Electronic filters rejected all the high-frequency noise in the bending-moments record at stations 5, 7½, 10, and 12½. The bending-moment record for station 15, which did not have a filter, had a small noise content which was smoothed out by eye when the record was analyzed.

All the data were non-dimensionalized in the process of data reduction. The wave heights were non-dimensionalized by dividing them by wave lengths, and were presented as wave steepness. Bending moment was converted to the non-dimensional coefficient  $\mu$  by dividing by the quantity  $\rho g L^3 B$ , where  $\rho g$  is the weight density of water,  $L$  is the model length, and  $B$  is the maximum model beam.

Irregular-Wave Test

The magnetic-tape records were processed by analog computer to obtain energy spectra of wave height and bending moments. This work was performed by Electronic Associates, Inc., at their computation center in Princeton, New Jersey. The computer output was in the form of tables of spectral densities of wave height,  $S_w$ , and bending moment (hog plus sag),  $S_M$ , at discrete frequencies. Bending-moment response amplitude operator, RAO, was obtained at each frequency by:

$$RAO = \frac{S_M}{S_w} \frac{(ft-ton)^2}{ft^2}$$

Bending-moment response,  $\sqrt{RAO}$  (ft-ton/ft), was then calculated and plotted versus frequency of wave encounter.

Where two runs were taken at a given speed to obtain a longer sample, two-run averages of wave spectral density  $(S_w)_a$  and bending-moment spectral density  $(S_M)_a$  at each frequency were calculated. The average RAO was then  $(S_M)_a / (S_w)_a$

The forward speed runs in following seas (zero-degree heading) were not spectrally analyzed, since the narrow range of low frequencies of encounter would have given rise to difficulties in interpreting the results.

Data Presentation

Regular Waves

The basic data for Model 2681-2 are presented in the form of a graph for each combination of model heading, speed, and wave length  $\lambda$ . Each graph shows the curves of variation in bending-moment coefficients  $\mu_{sag}$  and  $\mu_{hog}$  ( $\mu = \text{moment}/\rho g L^3 B$ ) along the hull length, for a series of constant values of wave steepness  $h/\lambda$ . These graphs appear in Figs. 6 to 26, with the exception of Fig. 14, which shows  $\mu_s$  and  $\mu_h$  versus  $h/\lambda$ .

It is necessary to bear in mind that  $\mu_s$  and  $\mu_h$  refer to dynamic bending moments and that the origin of the graphs is the still-water, zero-speed bending moment (Fig. 3).

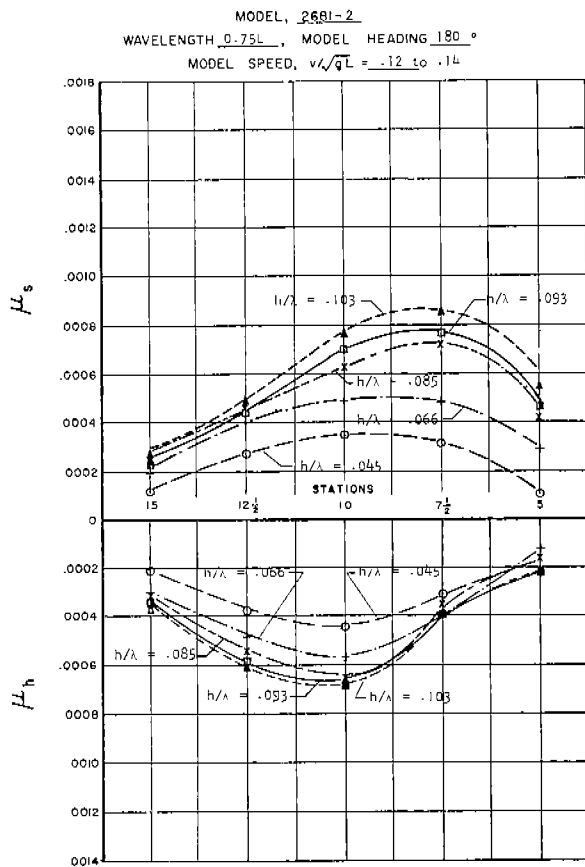


Fig. 6 Bending Moments Variation Along The Model Length.

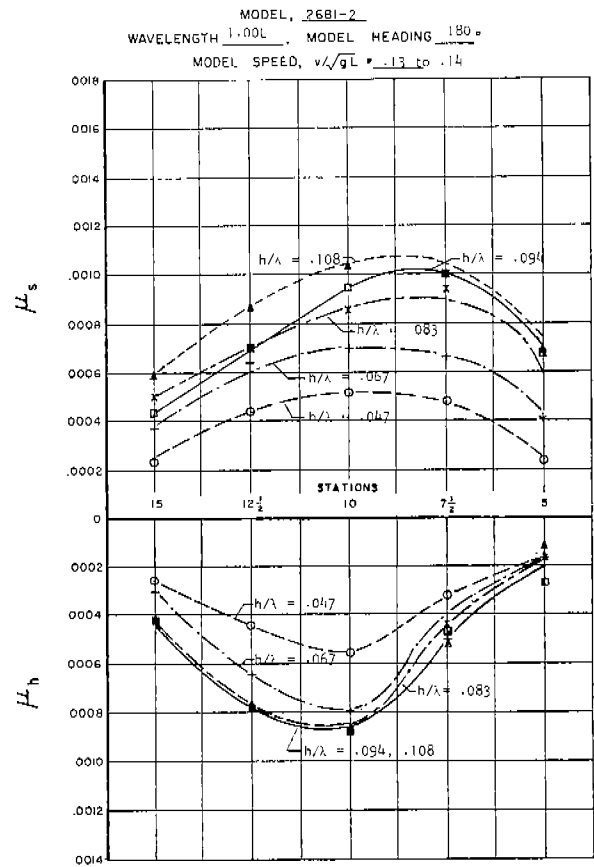


Fig. 7 Bending Moments Variation Along The Model Length.

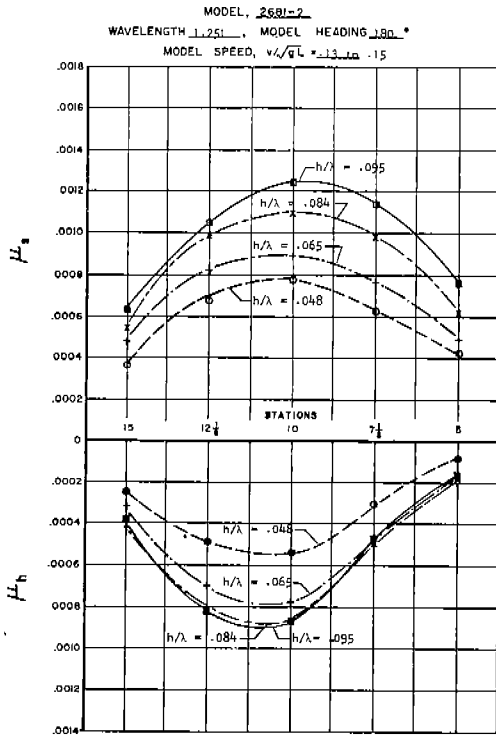


Fig. 8 Bending Moments Variation Along The Model Length.

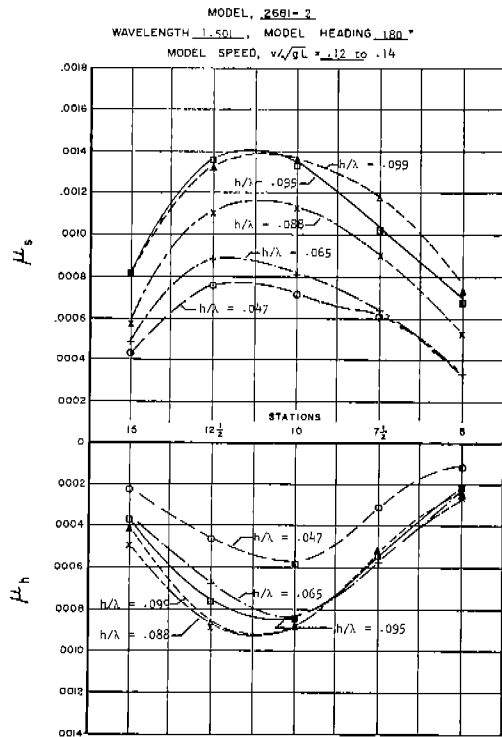


Fig. 9 Bending Moments Variation Along The Model Length.

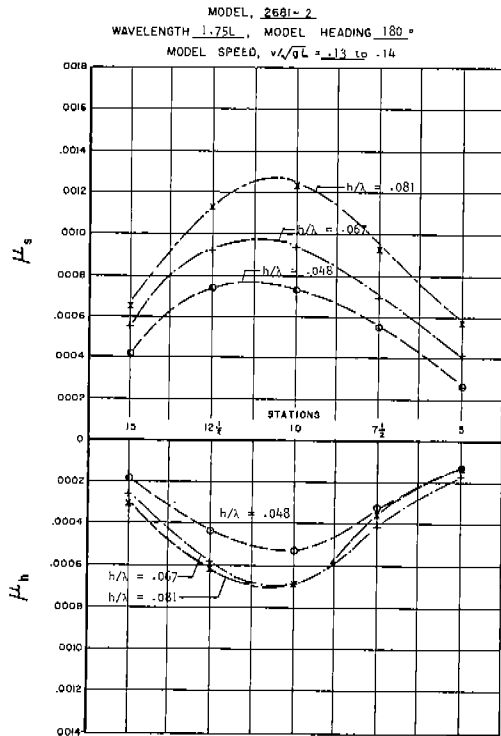


Fig. 10 Bending Moments Variations Along The Model Length.

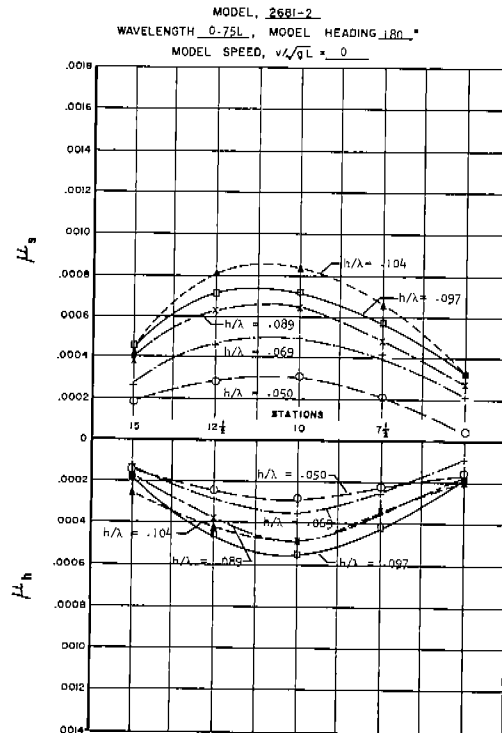


Fig. 11 Bending moments Variation Along The Model Length.

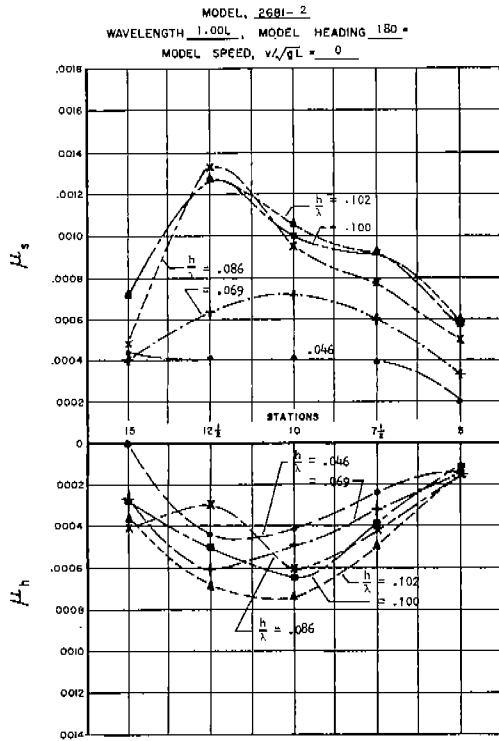


Fig. 12 Bending Moment Variation Along The Model Length.

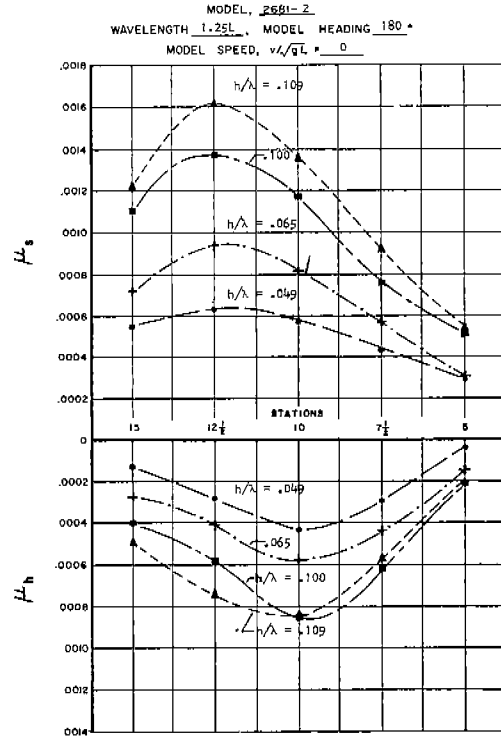


Fig. 13 Bending Moments Variation Along The Model Length.

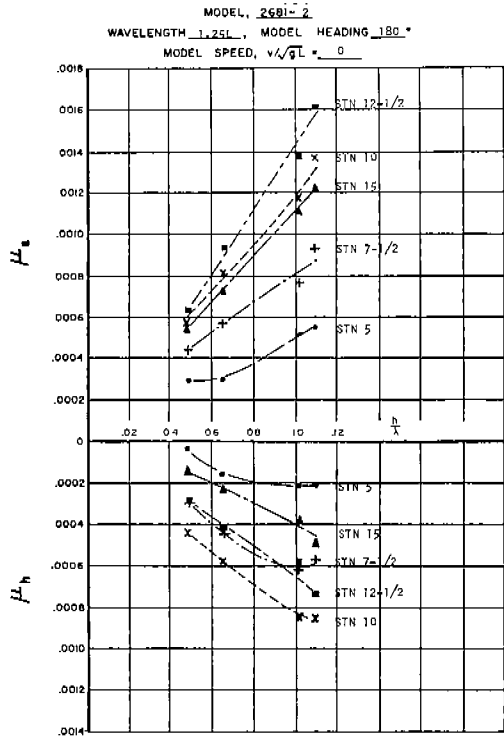


Fig. 14 Bending Moment Variation With Wave Height.

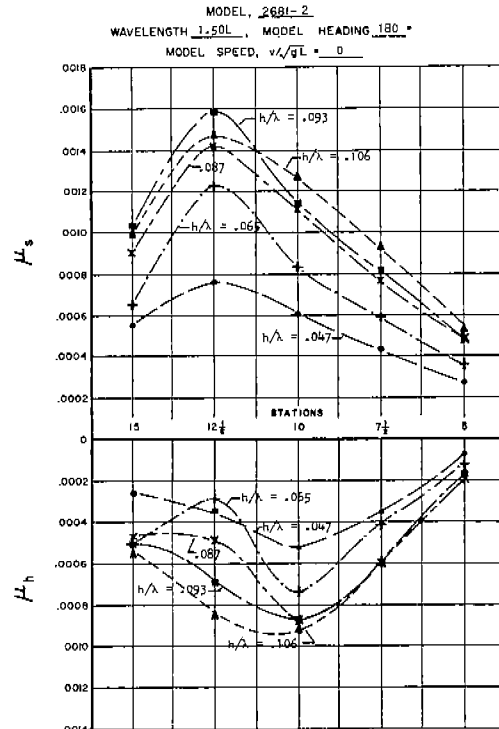


Fig. 16 Bending Moments Variation Along The Model Length.

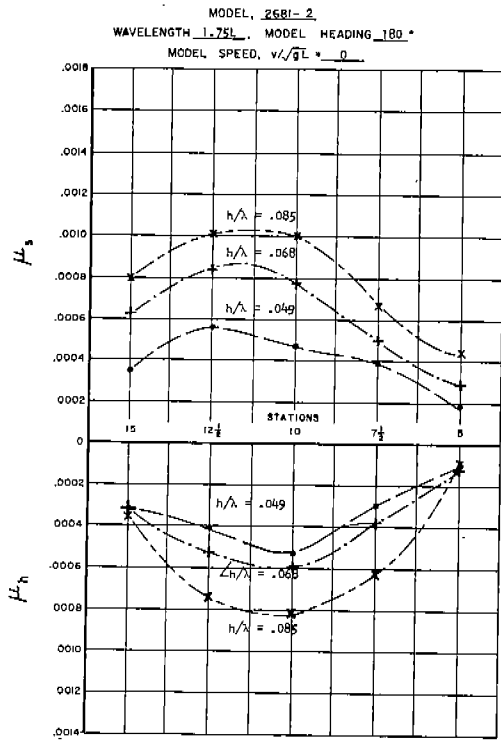


Fig. 16 Bending Moments Variation Along The Model Length.

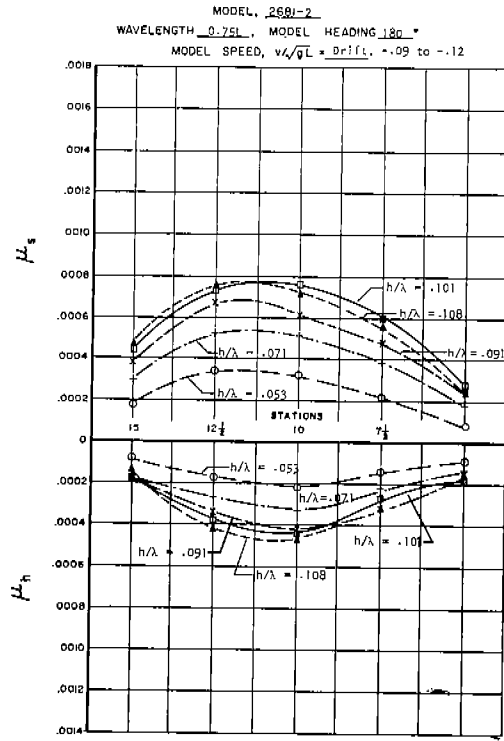


Fig. 17 Bending Moments Variation Along The Model Length.

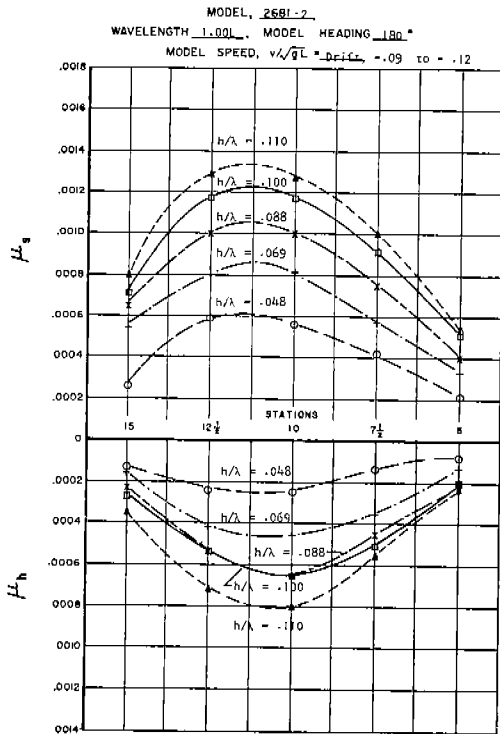


Fig. 18 Bending Moments Variation Along The Model Length.

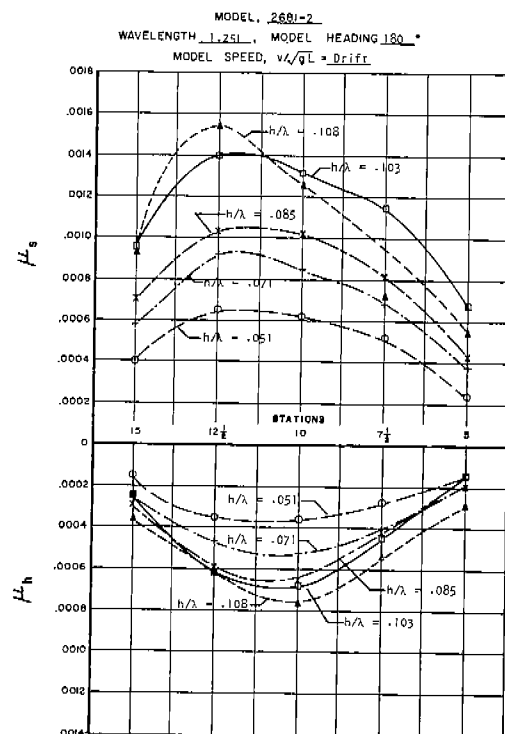


Fig. 19 Bending Moments Variation Along The Model Length.



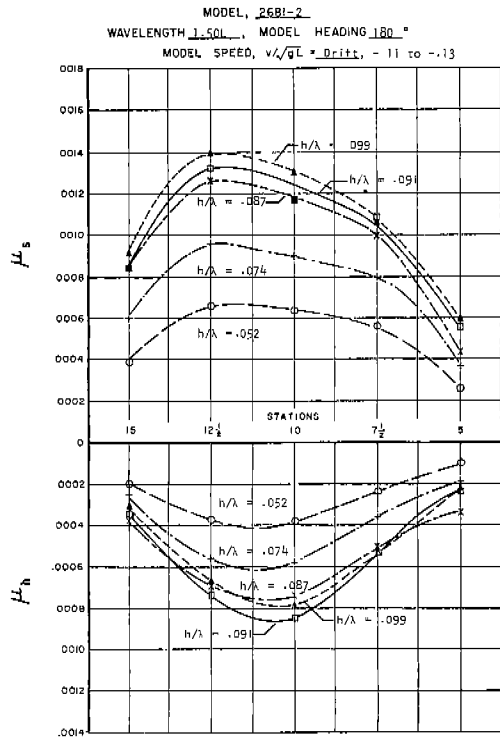


Fig. 20 Bending Moments Variation Along The Model Length.

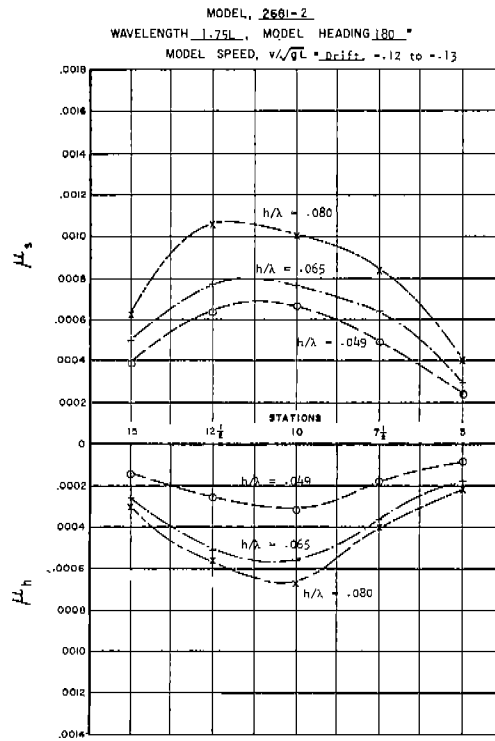


Fig. 21 Bending Moments Variation Along The Model Length.

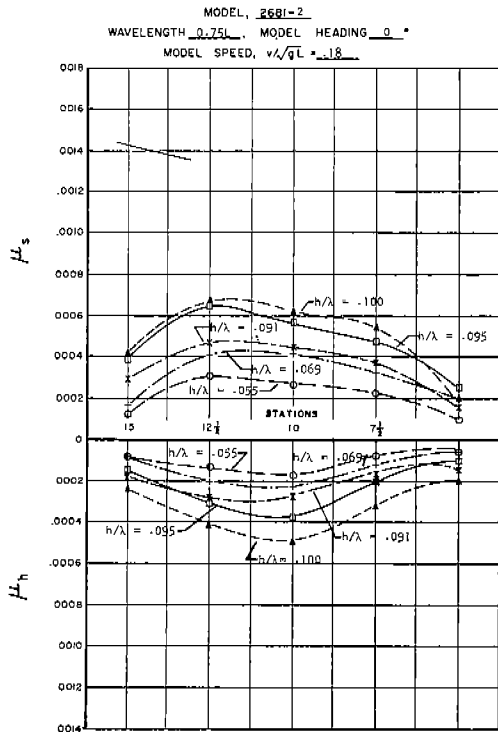


Fig. 22 Bending Moments Variation Along The Model Length.

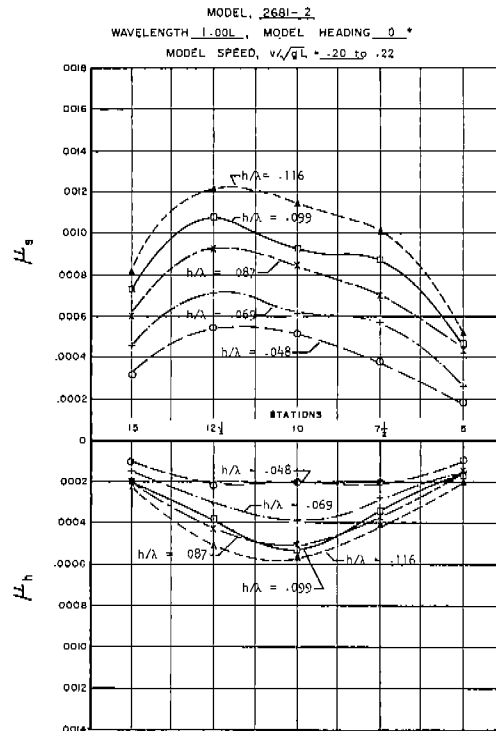


Fig. 23 Bending Moment Variation Along the Model Length.

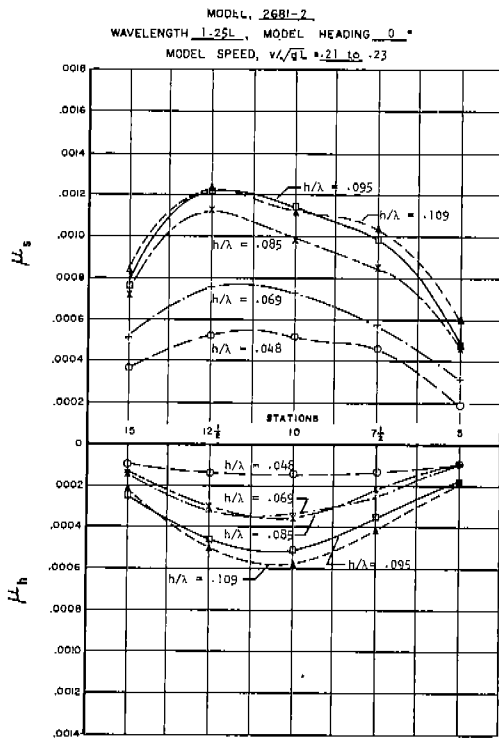


Fig. 24 Bending Moments Variation Along The Model Length.

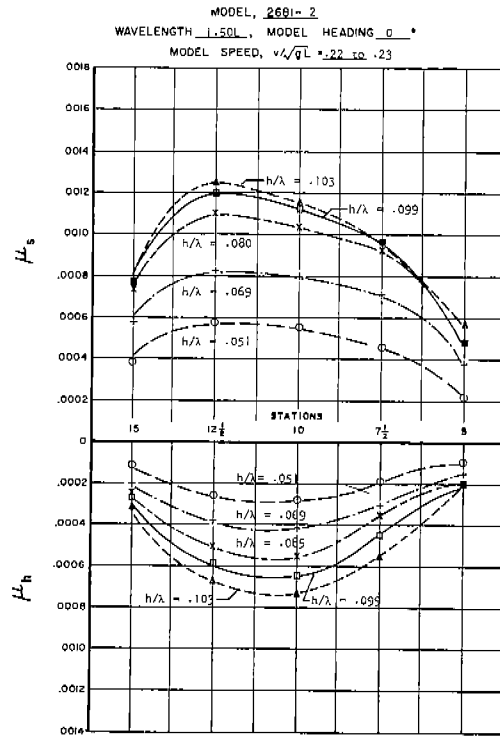


Fig. 25 Bending Moments Variation Along The Model Length.

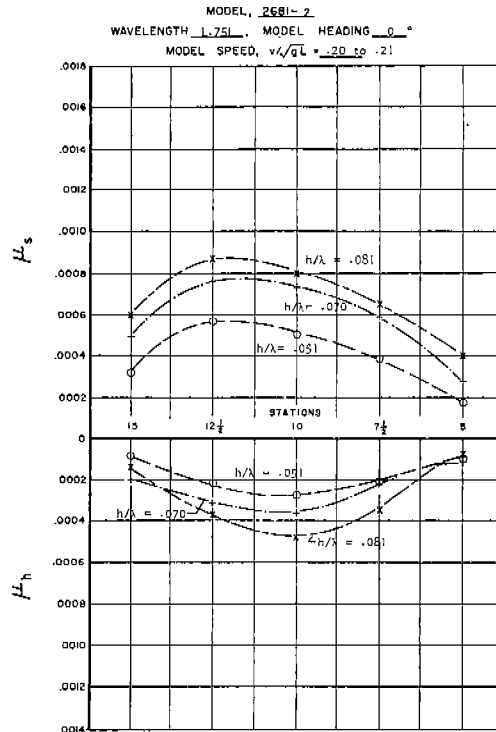


Fig. 26 Bending Moments Variation Along The Model Length.

MODEL 2681-2

L =  $h/\lambda < 0.07$   
 H =  $h/\lambda > 0.07$

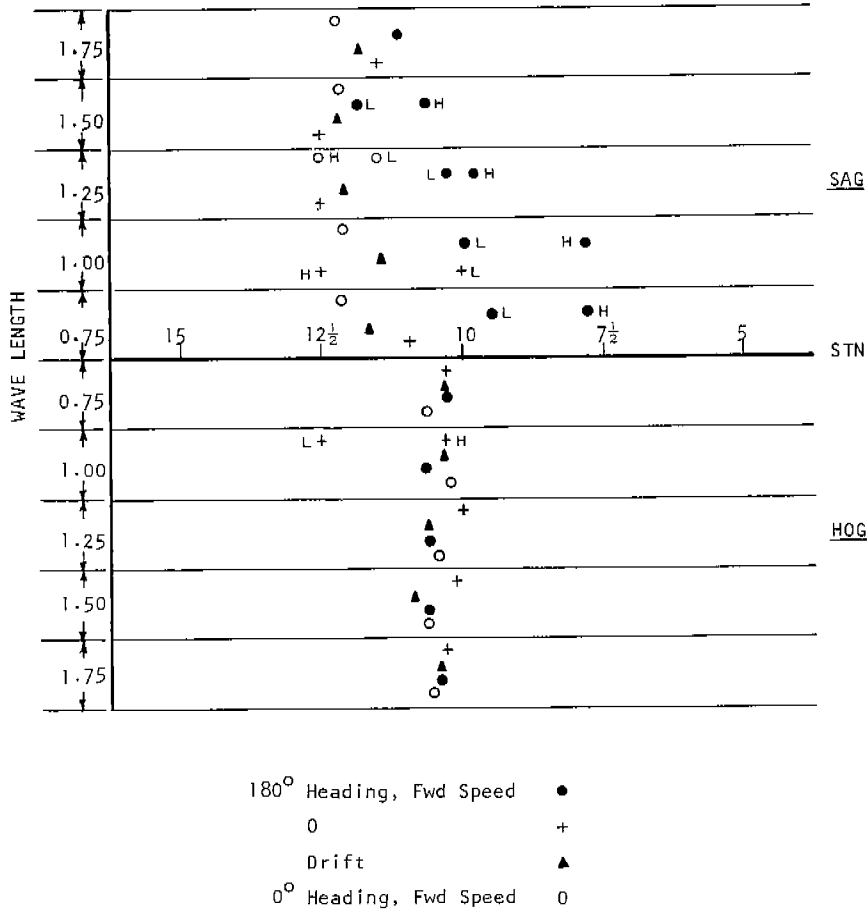


Fig. 27 Location Of Bending Moments Maxima.

Figure 27 shows the location of bending-moment maxima along the hull length during each different condition of heading, speed, and wave length. For constant  $h/\lambda = 0.05, 0.07, \text{ and } 0.10$ , the values of maxima appear in Figs. 28, 29, and 30, respectively.

Model 2681-2  
BOTH HEADINGS AND ALL SPEEDS

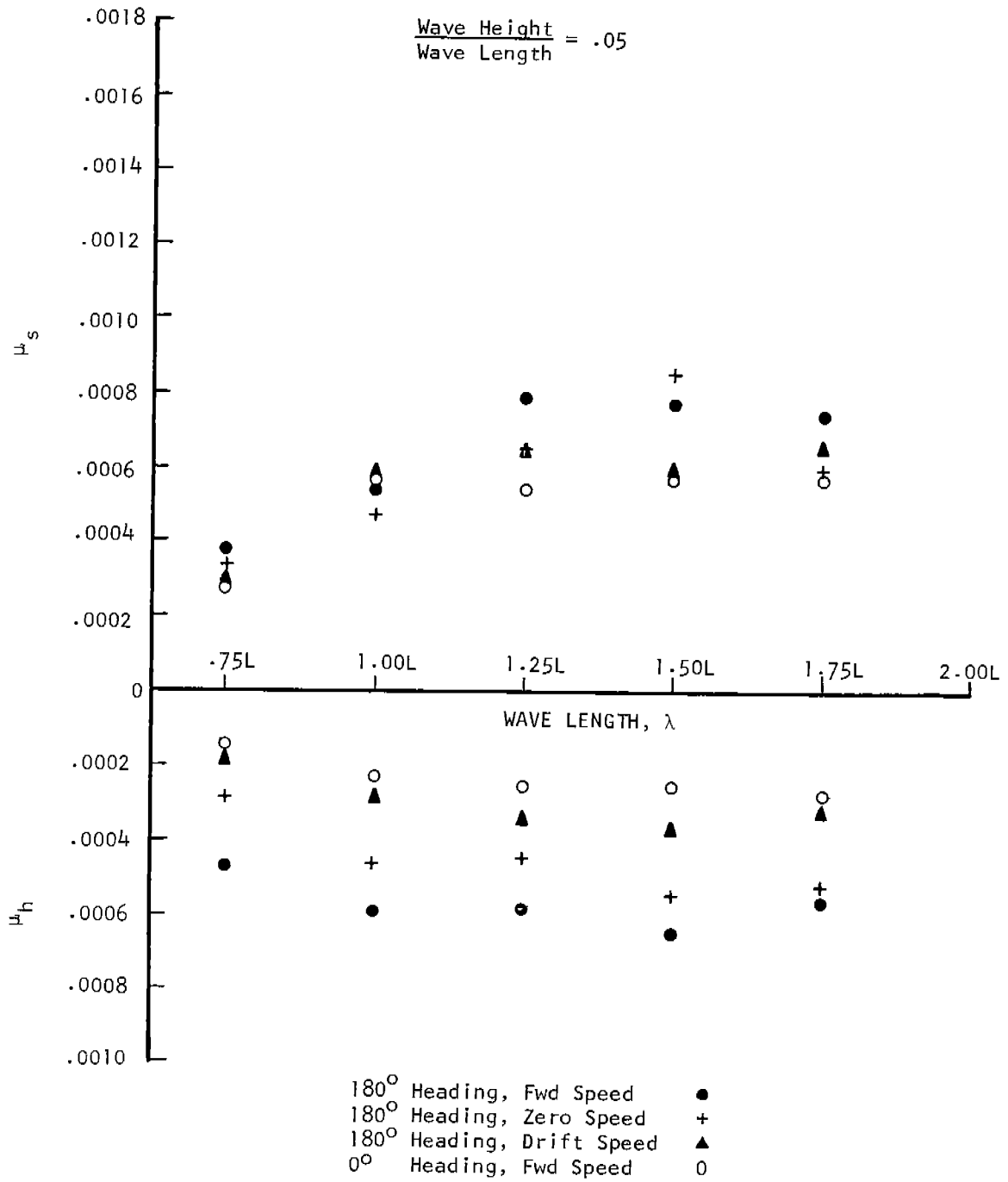


Fig. 28 Maximum Bending Moments Variation With Wave Length.

Model 2681-2

BOTH HEADINGS AND ALL SPEEDS

$$\frac{\text{Wave Height}}{\text{Wave Length}} = .07$$

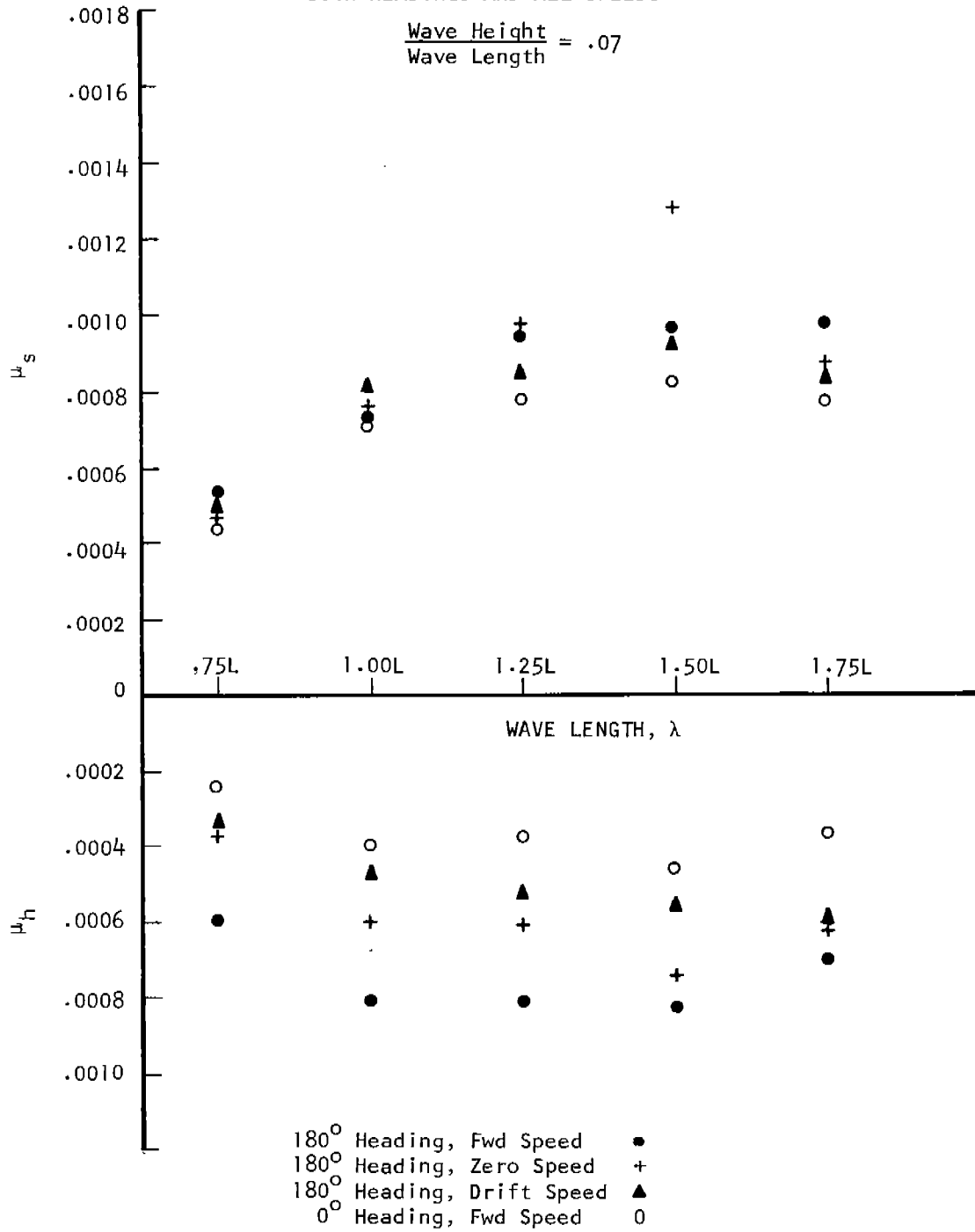


Fig. 29 Maximum Bending Moments Variation With Wave Length.

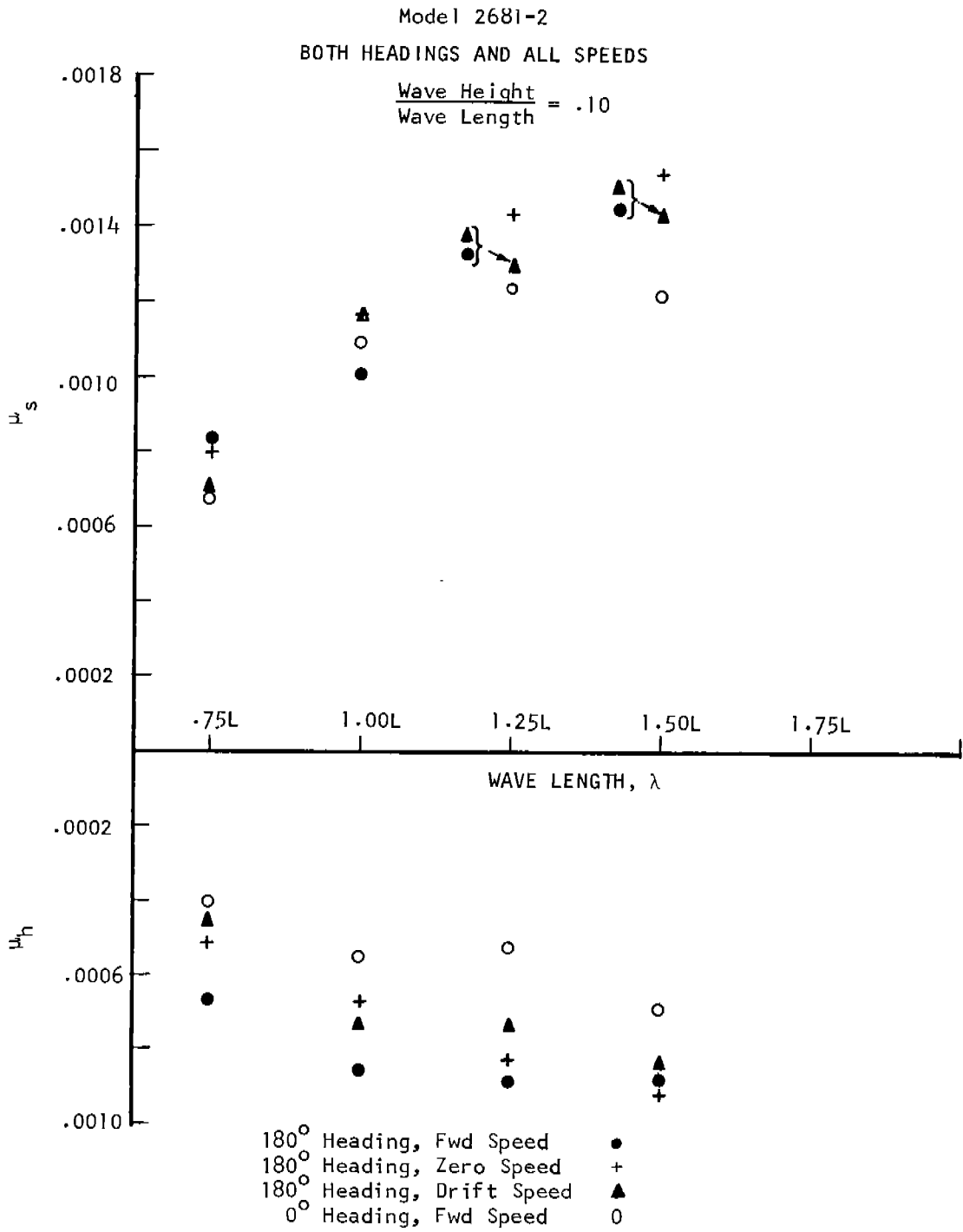


Fig. 30 Maximum Bending Moments Variation With Wave Length.

Model 2681-2  
Station 5  
BOTH HEADINGS AND ALL WAVE LENGTHS AND SPEEDS

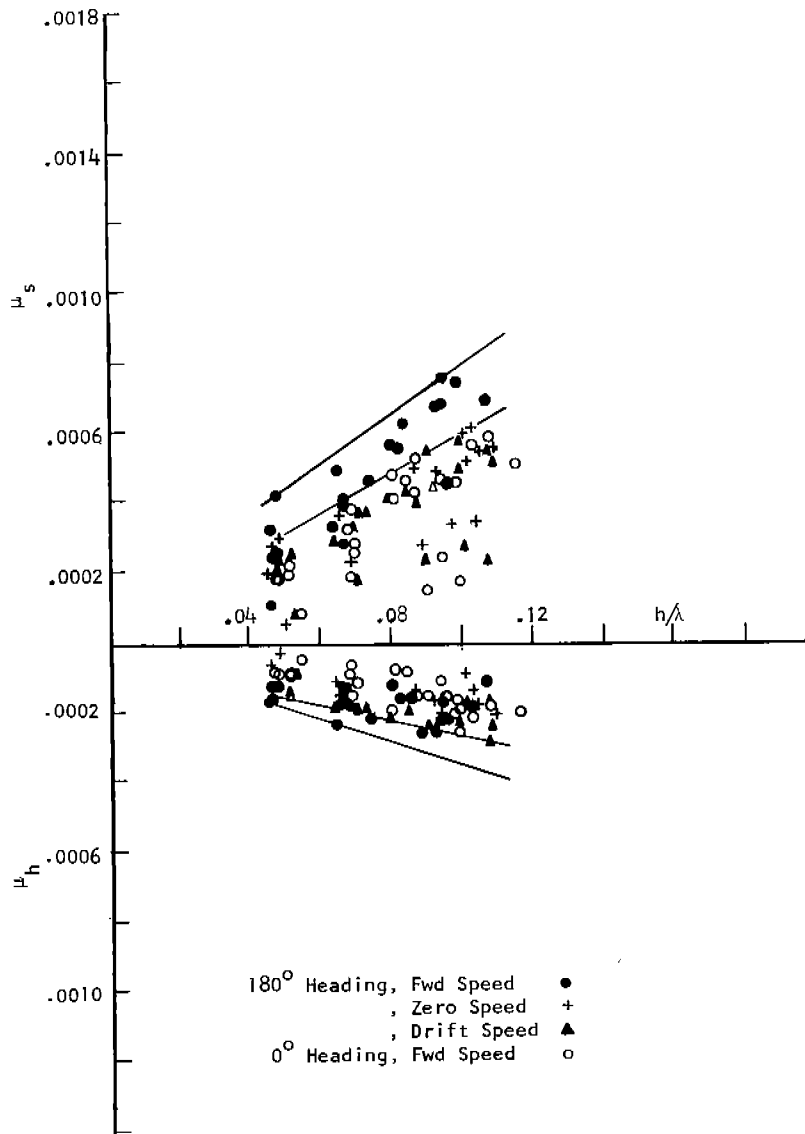


Fig. 31 Bending Moments Variation With Wave Steepness.

For an over-all view of bending-moment trends with wave height, all the data points of each test station are plotted on a single graph of  $\mu$  versus  $h/\lambda$  (Figs. 31 through 35). Four different symbols are used to distinguish between data for the four basic heading and speed conditions. Two envelopes are drawn to the scatter of the data; one includes all the data and one excludes data of the head-seas forward-speed case.

Model 2681-2  
Station 7 $\frac{1}{2}$   
BOTH HEADINGS AND ALL WAVE LENGTHS AND SPEEDS

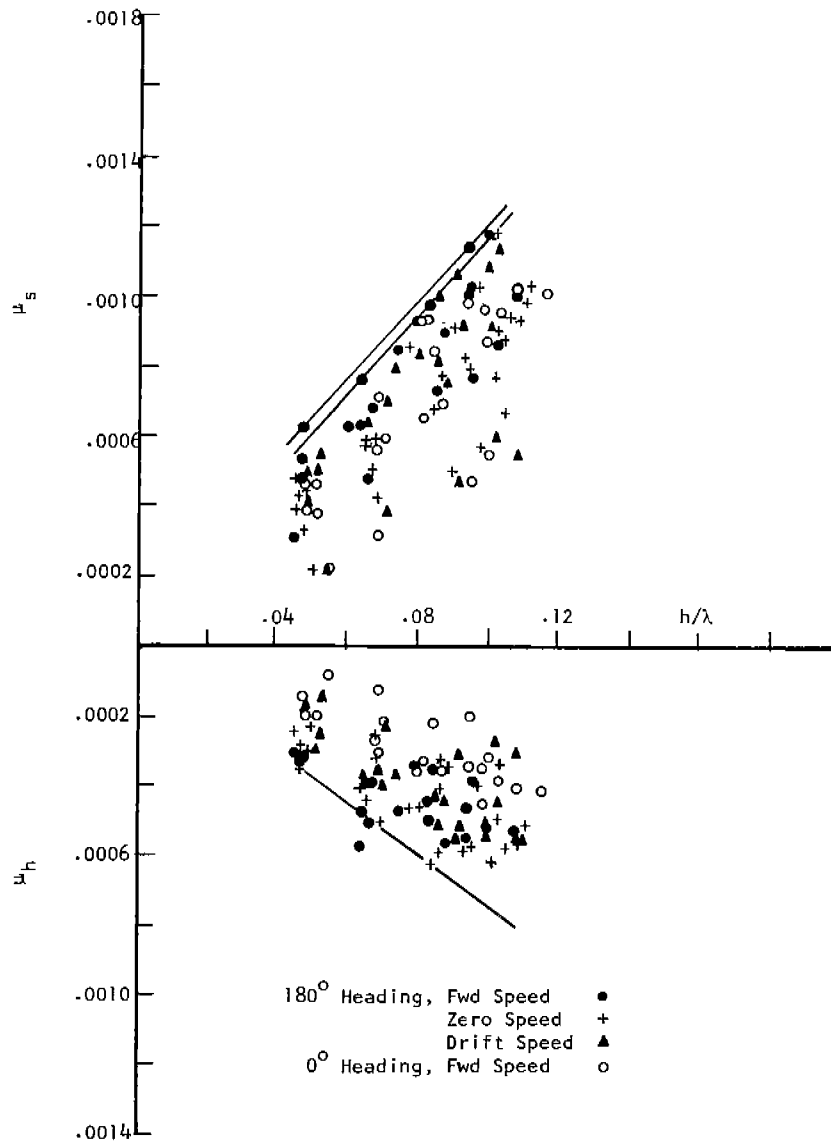


Fig. 32 Bending Moments Variation With Wave Steepness.

The data for the head-seas, zero-speed case in wave lengths 1.00L to 1.75L, which were obtained in the 1963 tests, are reproduced from Reference 4.



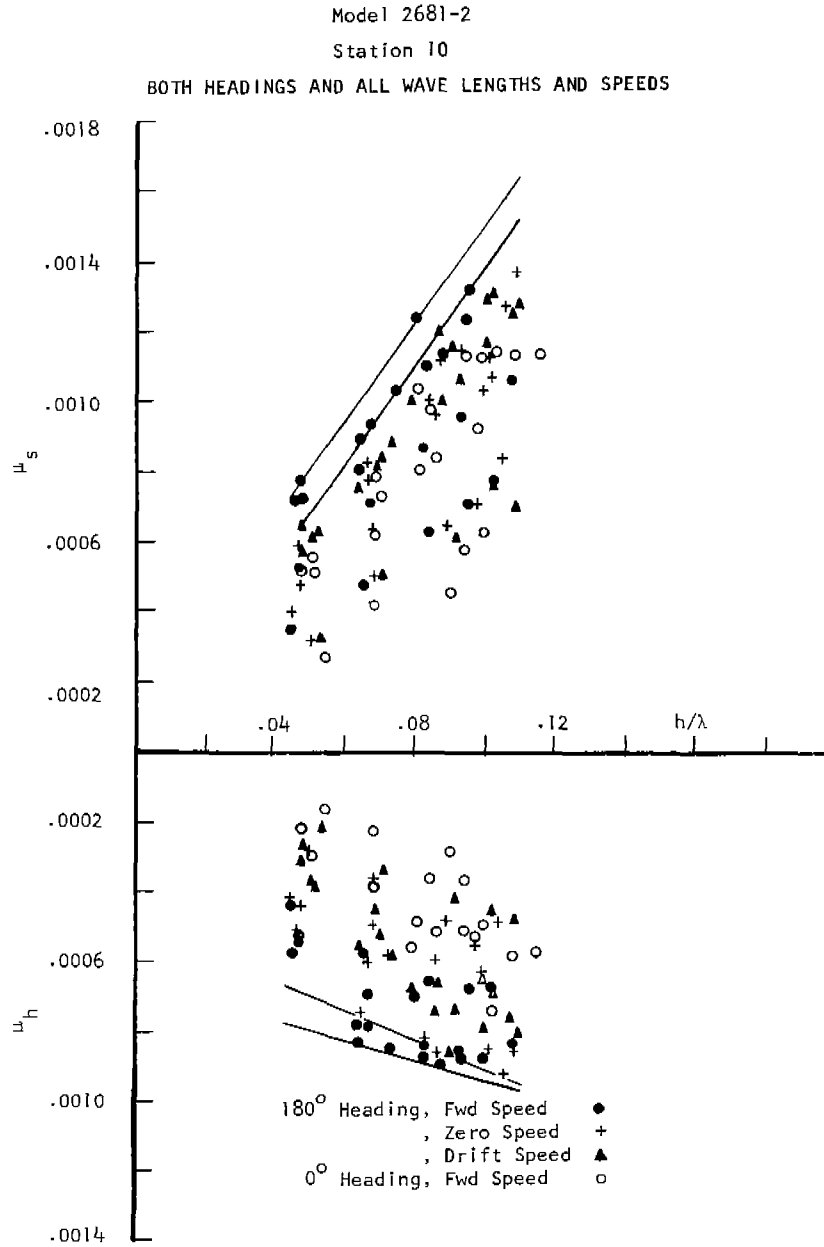


Fig. 33 Bending Moments Variation With Wave Steepness.

### Irregular Waves

Curves of bending-moment response ( $\sqrt{S_M/S_W}$ , ft-ton/ft) which were derived from the energy spectra have been charted on a base of wave frequency of encounter. Superimposed on each plot are bending-moment response points from regular-wave test data. These points represent the sum of hog and sag moments divided by wave height

Model 2681-2  
Station 12 $\frac{1}{2}$   
BOTH HEADINGS AND ALL WAVE LENGTHS AND SPEEDS

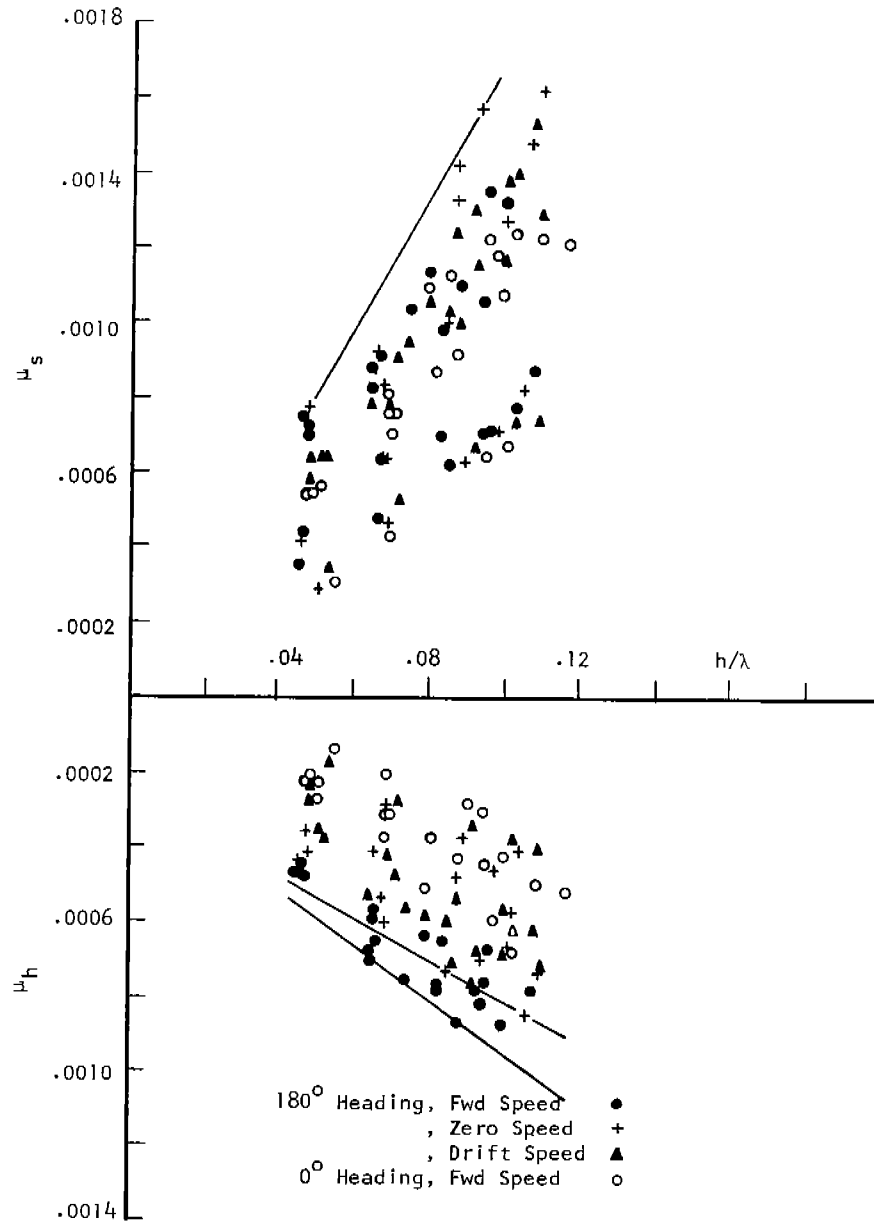


Fig. 34 Bending Moments Variation With Wave Steepness.

at  $h/\lambda = 0.08$ . This height/length ratio was chosen as being in the middle of the test range of wave steepness. Figures 36 and 37 present all such plots for model condition 2681-1 and 2681-2, respectively, within a matrix of speeds and hull stations.

Model 2681-2  
Station 15  
BOTH HEADINGS AND ALL WAVE LENGTHS AND SPEEDS

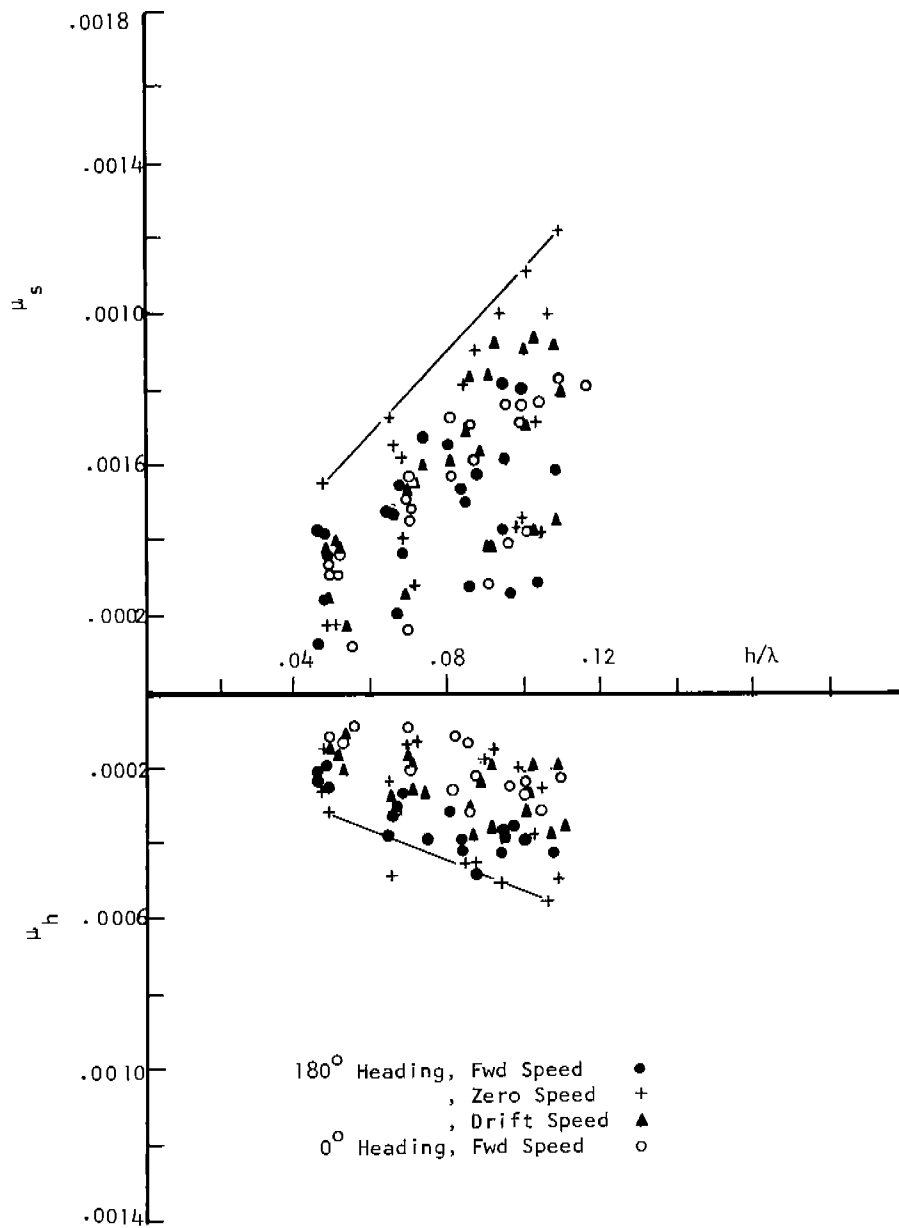


Fig. 35 Bending Moments Variation With Wave Steepness.

ANALYSIS AND DISCUSSION

The regular-wave data are discussed in the following sequence: (a) cargo-amidship case; (b) comparison of model with cargo amidship and model with normal weight distribution; (c) comparison of station 10 data for this test and Dalzell's test;<sup>2</sup> and (d) comparison between regular-wave and irregular-wave data.

— Derived from Spectra from Irregular Wave Tests  
 · · Regular Wave Results

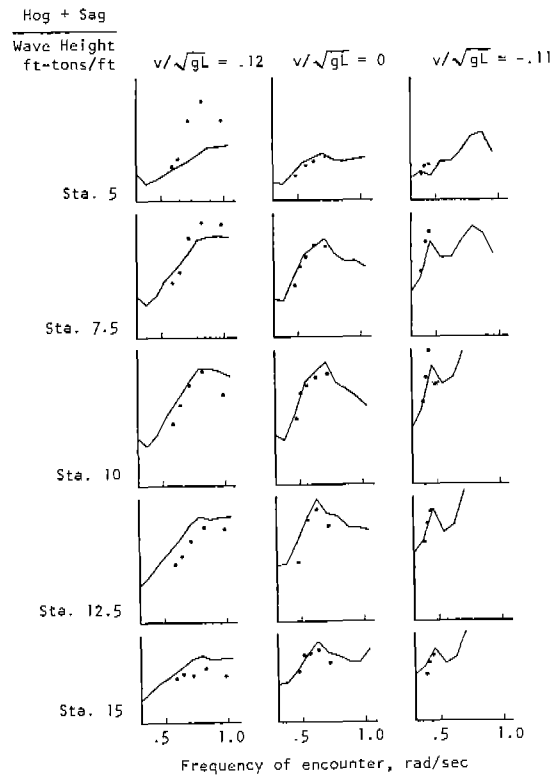


Fig. 36 Comparison Of Bending Moment Responses Normal Weight Distribution.

The measured moments are dynamic moments. The still-water bending moment coefficients are shown below.

Station	15	12½	10-(Ø)	7½	5
Normal-weight distribution	0.00022 hog	0.00040 hog	0.00047 hog	0.00043 hog	0.00029 hog
Cargo amidship	0.00004 sag	0.00039 sag	0.00053 sag	0.00013 sag	0.00007 hog

The static wave moments calculated without correction for Smith effect, at midship in a standard L/20 wave, are 0.00078 sag and 0.00059 hog.

Cargo-Amidship Weight Distribution

Speed range, and the location and wave length in which the maximum moments occur for various combinations of speed and model direction, are plotted in Fig. 27.

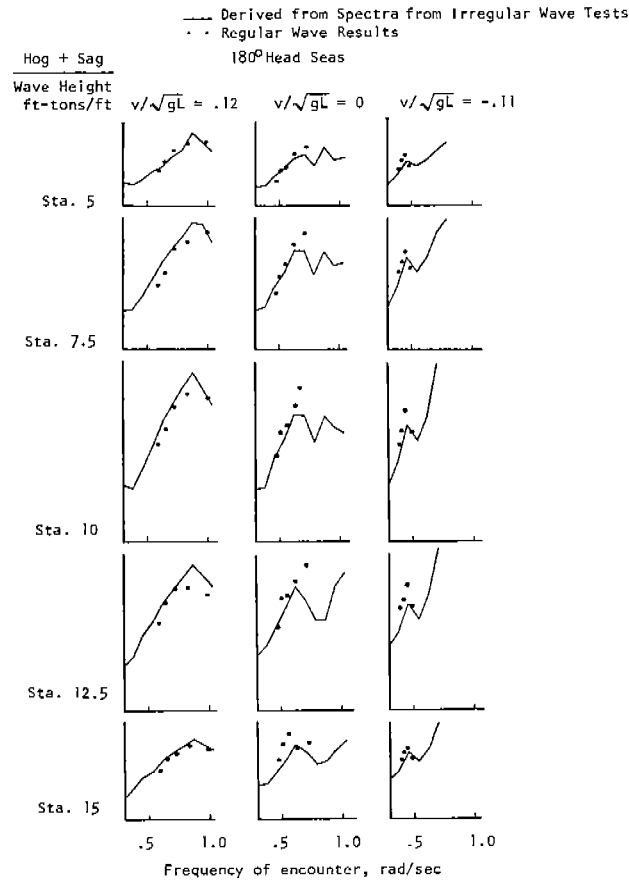


Fig. 37 Comparison Of Bending Moment Responses  
Cargo-Amidship Weight Distribution.

It is important to recognize that forward speeds of 9 to 11 knots in head seas and 14 to 18 knots in following waves would be impossible for the ship to realize in the more severe sea conditions simulated during the test. The installed horsepower of the MARINER is such that only the conditions of zero speed and drift speed could be maintained in the steepest waves.

Except in the case of head seas at forward speed in relatively short waves, the maximum sagging moments are located between stations 11 and 12½. The maximum hogging moments are located between stations 10 and 11¼ (see Fig. 27).

Figures 28-30 show that the maximum moments do not vary appreciably with wave length for wave lengths above 1.00L, except at zero speed. Generally, it may be said that the maximum moments occur in 1.25L to 1.75L wave lengths.

A complete set of charts showing curves of bending-moment coefficient versus wave height/length ratio was presented in the report<sup>2</sup> on the normal weight distribution. In the interests of streamlining the present report, only one such chart for the cargo-amidship case is shown, for illustrative purposes. Figure 14 is representative of the trends for the 180-degree heading at zero speed and drift speed, which are the only attainable speeds in the highest waves, as previously noted. It can be seen that both hog- and sag-moment coefficients are roughly proportional to wave height at all five locations. An alternative interpretation is

that there is no tendency for moments to reach an upper bound.

Generally, the dynamic sagging moments are larger than the dynamic hogging moments. In the midship area, high still-water sagging moments are present which, when added to the dynamic sagging moments, result in very large sagging moments.

Figures 31 to 35 present all the data collected at each test station. These figures are intended to compare at a glance the magnitude of moments in the four conditions of speed-heading combinations. The largest moments occur in head seas, mostly at forward or zero speeds. At stations 5,  $7\frac{1}{2}$ , and 10, the highest sagging moments occur at forward speed, while at stations  $12\frac{1}{2}$  and 15 they are found at zero speed. In the case of hogging moment, maximum moments of similar magnitudes occur at forward and zero speeds in head seas. This leads to the conclusion that, if the forward speed is considered unattainable, then the highest moment occurs at zero speed. However, it should be noted that the maximum moments in the drift-speed case and the following-seas case are not significantly smaller than in the case of forward speed and zero speed in head seas.

Comparison of Results for Normal Weight Distribution and Cargo Amidship  
(Magnitude of Moments)

An examination of the data for the two models reveals that the dynamic moments are not necessarily always larger or smaller for one model in comparison with the other. Gross estimate of tendencies is summarized below in table form. A mark, "x," appears against the model which has the larger moment; an "x" against both models means that the moments are of the same magnitude, or do not show a clear tendency.

Heading & Speed →		MAXIMUM MOMENT			
		180°, Fwd	180°, Zero	180°, Drift	0°, Fwd
Hog	Normal			x	x
	Cargo amidship	x	x		
Sag	Normal	x			
	Cargo amidship	x	x	x	x

The cargo-amidship case has generally larger sagging moments than the normal-weight-distribution case. Since dynamic sagging moments are larger than dynamic hogging moments, and, furthermore, since there is a large still-water sagging moment associated with the cargo-amidship distribution, such a loading results in a significantly higher total moment than does a normal weight distribution. For example, in waves of  $h/\lambda = 0.10$ , at drift speed in head seas, the moment coefficients at station 10 are:

	<u>Normal Loading</u>		<u>Cargo-Amidship Loading</u>	
	Hog	sag	Hog	Sag
Highest dynamic	0.00087	0.00127	0.00083	0.00130
Still water	0.00047	0.00047	0.00053	0.00053
Total	0.00134	0.00080	0.00030	0.00183
Total hog plus sag	0.00214		0.00213	

Although the bending-moment ranges -- total hog plus sag -- are comparable for the two loadings, the cargo-amidship case has a total sag moment which is one-third larger than the total hog moment of the normal loading case. Thus, any tendency to concentrate loads near amidships appears undesirable from the point of view of bending loads. However, such a tendency, which is reflected in a reduced pitch radius of gyration, is known to have the beneficial effects of easing pitching and heaving and reducing speed loss in waves. Clearly, the naval architect and ship operator must be cognizant of the conflicting effects of this type of loading.

Whereas Model 2681-1 had sagging-moment maxima around station 10 and hogging-moment maxima around station  $12\frac{1}{2}$ , Model 2681-2 had sagging- and hogging-moment maxima around stations  $11\frac{1}{2}$  and  $10\frac{1}{4}$  respectively. However, the maximum moments for both of the models remain within the midship quarter length.

Comparison of Station 10 Results with Results of Reference 2

Comparison of wave bending moments at station 10 with Dalzell's midship-moment results indicates that --

(a) Neither of the two groups of test results is consistently higher or lower than the other.

(b) For the case of sagging moments, six out of twenty comparable sets of results showed differences of 6 percent or less; ten showed differences of between 6 percent and 12 percent; and the maximum deviation was 21 percent. Average deviations in head seas were 13 percent at forward speed, 6 percent at zero speed, and 6 percent at drift speed. In following seas, the average deviation was 7 percent.

(c) For the case of hogging moments, ten out of twenty comparable sets of results showed differences of 6 percent or less; six showed differences of between 6 percent and 12 percent; and the maximum deviation was 16 percent. Average deviations in head seas were 10 percent at forward speed, 6 percent at zero speed, and 3 percent at drift speed. In following seas at forward speed the average deviation was 10 percent.

If one considers that the two tests under comparison were performed on different models with different instrumentation, by different people, the results show satisfactory agreement. Visual comparison of the slopes of corresponding curves shows that the sagging-moment curves have generally the same slopes, while the hogging-moment slopes in Dalzell's results are slightly higher than those in the results reported here.

Comparison Between Regular and Irregular Wave Data

If a ship-wave system is linear, that is, if ship motion amplitude in waves of fixed length is proportional to wave amplitude, then the principle of linear superposition may be applied. The principle may be stated as follows, according to

Model 2681-1

Station 5

180° Heading;  $v/\sqrt{gL} = .12 - .14$

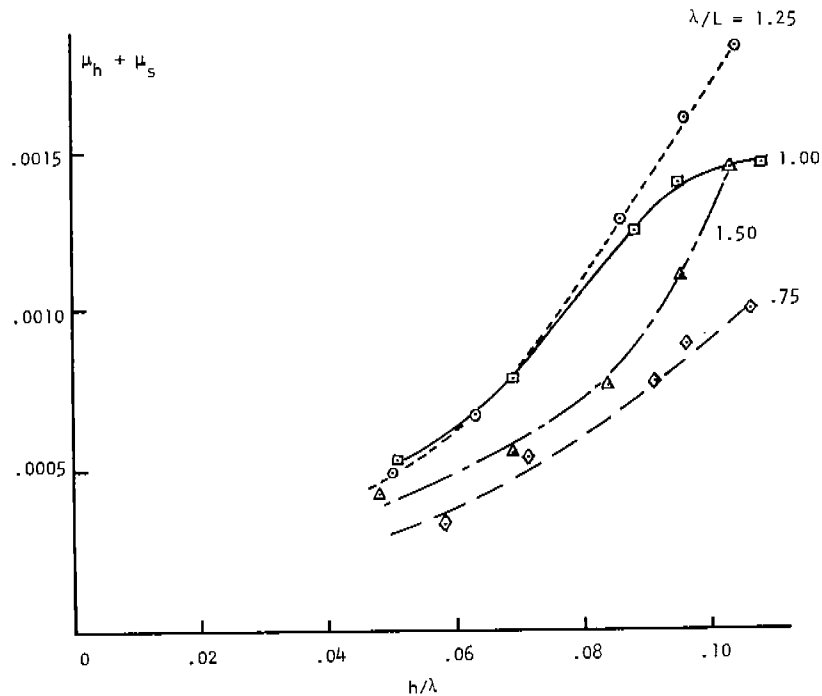


Fig. 38 Bending Moments Variation With Wave Height.

E. V. Lewis:<sup>5</sup> "The response of a ship to an irregular sea can be represented by a linear summation of its responses to the components of the sea." The components of the sea and the linear summation of ship responses are each defined by their respective energy spectra, for example the wave spectrum of Fig. 5.

In the present instance, tests of each loading condition in regular waves have yielded bending-moment results which are reasonably linear with wave height. Accordingly, the superposition principle can be applied and tested. A common method of testing the degree of applicability is to compare ship response functions (a) measured directly in regular waves and (b) derived from the relationship implicit in the superposition principle (response function times wave spectrum equals response spectrum) by obtaining the quotient (response spectrum divided by wave spectrum).

Figures 36 and 37 show that there is reasonable agreement between the results from the two sources. Only at station 5 for the normal loading at forward speed (Fig. 36) is there a consistent, significant difference. A possible explanation is that, in this case, significant forefoot emergence and slamming were detected in the regular-wave tests (see References 2 and 4). It is possible, therefore, that slamming augmented the bending moment in a non-linear manner, particularly at station 5, which was nearest to the region of impact. Figure 38 presents curves of bending-moment range (sag plus hog) at station 5 versus  $h/\lambda$ ; these curves show pronounced



non-linear trends at  $\lambda/L = 0.75, 1.00, \text{ and } 1.25$ . It is at these wave frequencies that the regular wave responses are significantly larger than the responses derived by spectral analysis of irregular-wave data.

Ochi,<sup>6</sup> also using the MARINER hull, showed that superposition technique is valid in rough seas if ship motion response functions are obtained from tests in regular waves of moderate height. To test this finding, the regular wave-bending-moment points for the case in question, Fig. 36, have been calculated from data from Fig. 38 at a moderate  $h/\lambda$  of 0.05 in the region where moment appears to be linear. These results are plotted on Fig. 39 and show better agreement with the response curve derived from irregular-wave tests than do the regular-wave points shown in Fig. 36; these latter results were calculated from data at an  $h/\lambda$  of 0.08, which is clearly in the non-linear range (see Fig. 38).

### Variation of Bending Moment Along Model Length

In Reference 4 it was shown that the MARINER with normal weight distribution, in head seas at drift speed and in following seas at forward speed, experienced unusual distributions of hogging moment along its length. The curves were characterized by distinct peaks at stations  $7\frac{1}{2}$  and  $12\frac{1}{2}$ , and this behavior remains unexplained.

Theoretical approaches predict the same wave bending moment for both sagging and hogging, whereas in the cases under question hogging and sagging moments have markedly different values as well as trends with location along model length.

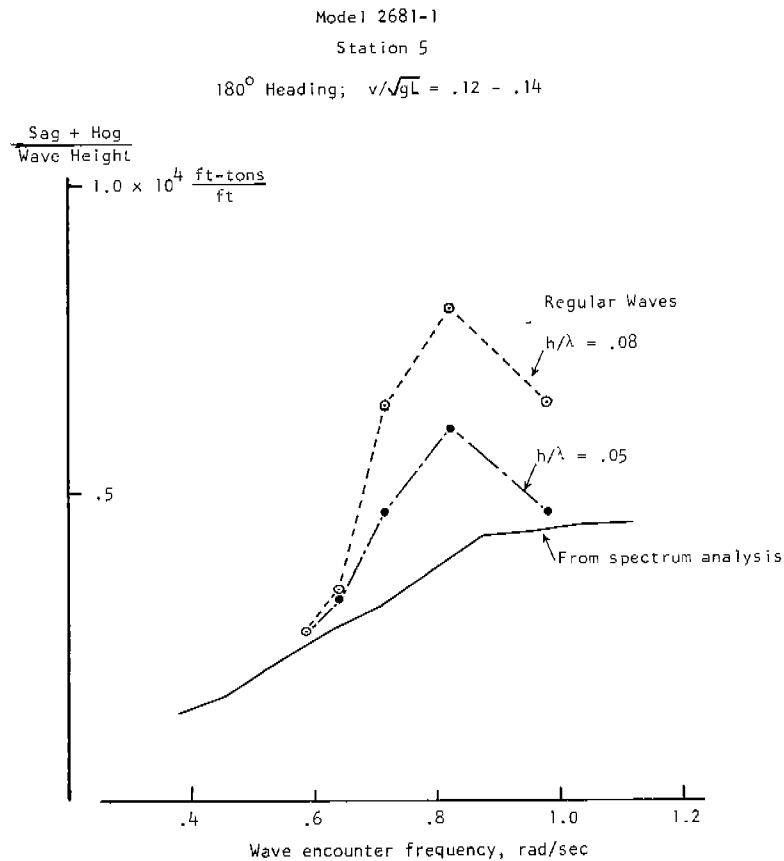


Fig. 39 Bending Moment VS. Wave Encounter Frequency.

In the test results for "cargo amidship" weight distribution (Figs. 6-26), there is no evidence of such a double-peak trend in any speed or heading condition, either in sagging or hogging.

#### SUMMARY

- (1) An extreme condition of weight distribution, denoted "cargo amidship," for the MARINER cargo ship running at speeds within practical operating limits in head and following seas, results in dynamic wave bending moments which --
  - (a) Reach peak values in regular waves of wave height/wave length ratios up to 0.11 between stations 10 and 12 $\frac{1}{2}$ .
  - (b) Are generally proportional to wave height up to a wave-height/wave-length ratio of 0.11.
  - (c) Are generally larger in sag than in hog and, when added to a sizable still-water sagging moment, result in a total sagging moment significantly larger than the total moment for a more normal weight distribution.
- (2) Tests of the MARINER hull with both a normal loading and the "cargo amidship" loading in high irregular head seas yield wave-bending-moment response curves which are in reasonable agreement with similar response results from regular-wave tests.

#### CONCLUSIONS

- (1) The practice of concentrating on midship bending moments both in design studies and full-scale measurements appears to be justified for ships of the MARINER type.
- (2) The good agreement between the irregular-wave and regular-wave responses inspires confidence in the use of regular-wave response operators and spectral-analysis technique to predict the vertical wave bending moment of a ship in irregular waves.

#### RECOMMENDATION

This broad investigation of wave bending moments acting on the hull girder of a MARINER cargo ship model has been actively continued over a period of approximately six years and is documented in a series of five technical reports.

The authors believe that significant trends of wave bending moment with wave steepness have been established, to the extent that further work in this area would yield diminishing returns. Efforts should now be directed toward checking model test results against the full-scale bending stress measurements collected under SR-153.

#### ACKNOWLEDGEMENT

The authors wish to thank the Ship Response Advisory Panel, headed by Mr. T. M. Buermann, for its guidance and encouragement during the planning, model testing, and data analysis phases of the project, 1964-1965.

REFERENCES

- (1) LEWIS, E. V. and Gerard, G., A Long-Range Research Program in Ship Structural Design. Ship Structure Committee, Serial SSC-124, November 1959.
- (2) DALZELL, J. F., An Investigation of Midship Bending Moments Experienced in Extreme Regular Waves by Models of the MARINER Type Ship and Three Variants. Ship Structure Committee, Serial SSC-155, January 1964.
- (3) DALZELL, J. F., An Investigation of Midship Bending Moments Experienced in Extreme Regular Waves by Models of a Tanker and a Destroyer. Ship Structure Committee, Serial SSC-156, February 1964.
- (4) MANIAR, N. M., Investigation of Bending Moments Within the Midship Half Length of a MARINER Model in Extreme Waves. Ship Structure Committee, Serial SSC-163, June 1964.
- (5) COMSTOCK, J. P. (ed.), Principles of Naval Architecture. Society of Naval Architects and Marine Engineers (SNAME), 1967; Chap. IX by E. V. Lewis, p. 660.
- (6) OCHI, K. M., "Extreme Behavior of a Ship in Rough Seas -- Slamming and Shipping of Green Water," Trans. SNAME, Vol. 72, 1964, p. 143.

UNCLASSIFIED

Security Classification

DOCUMENT CONTROL DATA - R & D

(Security classification of title, body of abstract and indexing annotation must be entered when the overall report is classified)

1. ORIGINATING ACTIVITY (Corporate author) Davidson Laboratory Stevens Institute of Technology		2a. REPORT SECURITY CLASSIFICATION Unclassified	
		2b. GROUP	
3. REPORT TITLE BENDING MOMENT DISTRIBUTION IN A MARINER CARGO SHIP MODEL IN REGULAR AND IRREGULAR WAVES OF EXTREME STEEPNESS			
4. DESCRIPTIVE NOTES (Type of report and, in r l sive dates) Final			
5. AUTHOR(S) (First name, middle initial, last name) Naresh M. Maniar Edward Numata			
6. REPORT DATE November 1968		7a. TOTAL NO. OF PAGES 33	7b. NO. OF REFS 6
8a. CONTRACT OR GRANT NO Nobs 88263		9a. ORIGINATOR'S REPORT NUMBER(S) 2882/233	
b. PROJECT NO. SF-0130304, Task 2022 SR-165		9b. OTHER REPORT NO(S) (Any other numbers that may be assigned this report) SSC-190	
c.			
d.			
10. DISTRIBUTION STATEMENT Distribution of this document is unlimited			
11. SUPPLEMENTARY NOTES		12. SPONSORING MILITARY ACTIVITY Ship Structure Committee Naval Ship Systems Command Department of the Navy Washington, D. C. 20360	
13. ABSTRACT An experimental investigation was undertaken to determine (1) the lengthwise vertical wave-bending-moment distribution within the midship half-length and (2) the relationship between bending moment and extreme wave steepness, for a MARINER-type cargo ship. A 1/96-scale model was cut to form six segments, which were joined by a flexure beam. The beam was strain-gaged to measure bending moments at the hull cuts at stations 5, 7 $\frac{1}{2}$ , 10, 12 $\frac{1}{2}$ , and 15. The model was tested with normal weight distribution and with an extreme "cargo amidship" loading in both head and following seas. The range of regular-wave steepness (height/length) was 0.05 to 0.11; the irregular waves had an equivalent full-size significant height of 39 feet. Within practical operational limits of speed for the MARINER-type ship, the maximum wave bending moments in high regular waves were found to occur in the region from amidships to 0.125L aft of amidships. Thus the practice of concentrating on midship bending moments both in design studies and full-scale measurements appears to be justified for ships of the MARINER type. Hogging and sagging moments at any section were found to be generally proportional to wave height, up to a wave-height to wave-length ratio of 0.11, the steepest wave that could be generated. The bending-moment and wave data from the tests in irregular waves were processed by spectral analysis to obtain equivalent regular-wave responses. These were shown to be, generally, in good enough agreement with the bending-moment responses obtained directly in regular waves to inspire confidence in the use of regular-wave response operators and spectral-analysis technique to predict the vertical wave bending moment of a ship in irregular waves.			

DD FORM 1473 (PAGE 1)  
1 NOV 65

S/N 0101-807-6811

UNCLASSIFIED  
Security Classification

A-31408

14 KEY WORDS	LINK A		LINK B		LINK C	
	ROLE	WT	ROLE	WT	ROLE	WT
Cargo Ship Ship Hulls Ship Bending Moment Model Tests Water Waves						

NATIONAL ACADEMY OF SCIENCES-NATIONAL RESEARCH COUNCIL

DIVISION OF ENGINEERING

*This project has been conducted under the advisory guidance of the Ship Research Committee of the National Academy of Sciences National Research Council. The Committee assumes such cognizance of projects in materials, design and fabrication as relating to improved ship structures, when such activities are accepted by the Academy and assigned through its Maritime Transportation Research Board. In addition, this committee recommends research objectives and projects; provides liaison and technical guidance to such studies; reviews project reports; and stimulates productive avenues of research.*

SHIP RESEARCH COMMITTEE

*Chairman:* M. L. Sellers, (I, II, III)  
Naval Architect  
Newport News Shipbuilding and Drydock Co.

*Vice Chairman:* J. M. Frankland (I, II, III)  
(Retired) Mechanics Division  
National Bureau of Standards

*Members*

William H. Buckley (I, II)  
Chief, Structural Criteria  
Bell Aerosystems Company

John E. Goldberg, (I, II)  
School of Civil Engineering  
Purdue University

B. B. Burbank (III)  
(Retired) Chief Metallurgist  
and Chemist  
Bath Iron Works Corp.

Joseph E. Herz (I, II)  
Chief Structural Design Engineer  
Sun Shipbuilding and Drydock Co.

D. P. Clausing (III)  
Senior Scientist  
U. S. Steel Corporation

G. E. Kampschaefer, Jr. (III)  
Manager, Application Engineering  
ARMCO Steel Corporation

D. P. Courtsal (II, III)  
Principal Hull Design Engineer  
Dravo corporation

Bryan R. Noton (II, III)  
Department of Aeronautics  
and Astronautics  
Stanford University

A. E. Cox (I, II)  
LHA Project Director  
Newport News Shipbuilding  
and Drydock Co.

Stanley T. Rolfe (III)  
Section Supervisor  
U. S. Steel Applied Research Center

F. V. Daly (III)  
Manager of Welding  
Newport News Shipbuilding and  
and Drydock Co.

Merville Willis (I)  
Assistant Naval Architect  
Sun Shipbuilding and Dry Dock Co.

John F. Dalzell (I)  
Senior Research Scientist  
Hydronautics Incorporated

R. A. Yagle (II)  
Department of Naval Architecture  
and Marine Engineering  
University of Michigan

*(I) - Advisory Group I, Ship Strain Measurement & Analysis*  
*(II) - Advisory Group II, Ship Structural Design*  
*(III) - Advisory Group III, Ship Metallurgical Studies*

R. W. Rumke  
*Executive Secretary*

## SHIP STRUCTURE COMMITTEE PUBLICATIONS

*These documents are distributed by the Clearinghouse, Springfield, Va. 22151. These documents have been announced in the Technical Abstract Bulletin (TAB) of the Defense Documentation Center (DDC), Cameron Station, Alexandria, VA. 22314, under the indicated AD numbers.*

- SSC-178, *A Survey of Some Recent British Work on the Behavior of Warship Structures* by J. Clarkson. November 1966. AD 644738.
- SSC-179, *Residual Strains and Displacements Within the Plastic Zone Ahead of A Crack* by J. Cammett, A. R. Rosenfield, and G. T. Hahn. November 1966. AD 644815.
- SSC-180, *Experimental Determination of Plastic Constraint Ahead of a Sharp Crack under Plane-Strain Conditions* by G. T. Hahn and A. R. Rosenfield. December 1966. AD 646034.
- SSC-181, *Results from Full-Scale Measurements of Midship Bending Stresses on Two Dry-Cargo Ships- Report #2* by D. J. Fritch, F. C. Bailey, J. W. Wheaton. March 1967. AD 650239.
- SSC-182, *Twenty Years of Research Under the Ship Structure Committee* by A. R. Lytle, S. R. Heller, R. Nielsen, Jr., and John Vasta. December 1967. AD 663677.
- SSC-183, *Metallurgical Structure and the Brittle Behavior of Steel* by Morris Cohen. May 1968. AD 670574.
- SSC-184, *Exhaustion of Ductility in Compressed Bars with Holes* by S. Kabayashi and C. Mylonas. June 1968. AD 670487.
- SSC-185, *Effect of Surface Condition On The Exhaustion Of Ductility By Cold or Hot Straining* by J. Dvorak and C. Mylonas. July 1968.
- SSC-186, *On the Effect of Ship Stiffness Upon the Structural Response of a Cargo Ship to an Impulsive Load* by Manley St. Denis. September 1968.
- SSC-187, *Biennial Report of Ship Structure Committee*, June 1968.
- SSC-188, *Effect of Repeated Loads On The Low Temperature Fracture Behavior Of Notched And Welded Plates*. W. H. Munse, J. P. Cannon and J. F. Kiefner. October 1968.
- SSC-189, *The Video Tape Recording of Ultrasonic Test Information* by Robert A. Youshaw, Charles H. Dyer and Edward L. Criscuolo. October 1968.
- SSC-190, *Bending Moment Distribution In a Mariner Cargo Ship Model In Regular and Irregular Waves of Extreme Steepness*. by Naresh M. Maniar and Edward Numata. November 1968.